

Throughput Estimation Models under Various
Conditions and MIMO Host Location Optimization
Approach for Wireless Local-Area Network

September, 2018

Sumon Kumar Debnath

Graduate School of
Natural Science and Technology

(Doctor's Course)
OKAYAMA UNIVERSITY

Dissertation submitted to
Graduate School of Natural Science and Technology
of
Okayama University
for
partial fulfillment of the requirements
for the degree of
Doctor of Philosophy.

Written under the supervision of

Professor Nobuo Funabiki

and co-supervised by

Professor Satoshi Denno

and

Professor Yasuyuki Nogami

OKAYAMA UNIVERSITY, September 2018.

TO WHOM IT MAY CONCERN

We hereby certify that this is a typical copy of the original doctor thesis of
Sumon Kumar Debnath

Signature of
the Supervisor

Seal of

Prof. Nobuo Funabiki

Graduate School of
Natural Science and Technology

Abstract

Recently, *Wireless Local-Area Networks (WLANs)* have become prevailing around the world due to the cost-effective, and flexible Internet access solution using wireless communications between user hosts and *access points (APs)*. For hosts in WLAN, typically personal computers (PCs) or other Wi-Fi devices such as smart phones or tablets are used. These hosts are usually located at fixed positions in indoor environments that may consist of several rooms for offices, laboratories, or classrooms in a company or a university, because users are using them on tables while sitting on chairs. Multiple APs are often installed in the network field, which may cause the poor performance due to interferences among them. Besides, the number of communicating hosts may fluctuate with time of a day or a week. The network configuration of WLAN should be properly adapted to these changes.

Previously, we have studied the *elastic WLAN system* and proposed the *active AP configuration algorithm* as a solution to the aforementioned problem. This algorithm optimizes the network configuration of WLAN by dynamically activating/deactivating APs, assigning the channels to the active APs, and changing the host associations, depending on the network situation. Unfortunately, the current active AP configuration algorithm assumes the *single-input-single-output (SISO)* link with a single antenna for any host. Nowadays, the *multiple-input-multiple-output (MIMO)* link with multiple antennas has become popular as the faster communication technology in commercial AP devices and high-class PC models.

Under current situations, a lot of commercial APs have adopted MIMO, and only the limited number of hosts can use MIMO due to the cost reason. In this study, a host adopting MIMO is referred to as a *MIMO host*, and a host with only SISO is as a *SISO host* for convenience. Then, the proper location of the limited MIMO hosts in the network field becomes critical to improve the communication performance by utilizing the potential ability of MIMO communications. At the same time, the accurate throughput estimation of a MIMO/SISO link also becomes important in this MIMO host location optimization.

In this thesis, first, to study the *throughput estimation model*, we present throughput measurement results of WLAN under various conditions both in indoor and outdoor environments. In these measurements, we adopt commercial dedicated APs and software APs using Raspberry Pi for APs, and PCs with IEEE 802.11n MIMO and SISO links for user hosts. Here, we consider both cases: 1) a single host communicates with an AP at a time, and 2) multiple hosts communicate with a single AP at a time (concurrent communications). The results show that *RSS (Receive Signal Strength)* and the throughput of a host is strongly affected by the type of the AP or PC, the link distances, and the network environment. Then, based on throughput measurement results, we extend the previous throughput estimation model, particularly to consider the concurrent communications of multiple hosts. The comparisons of the estimated throughput and the measured one support the correctness of our proposal.

Next, we present the extension of the active AP configuration algorithm to optimize the *MIMO host location* for the elastic WLAN system by considering the effects in concurrent communication. In this extension, the MIMO host locations are optimized by repeatedly swapping the location of a SISO host and that of a MIMO host for fixed times, if the result satisfies the constraints for the network and improve the total throughput performance. The effectiveness of this proposal has been verified through simulations in two network topologies using the WIMNET simulator and simple testbed experiments.

In future studies, we will consider further enhancements to the throughput estimation model and the MIMO host location optimization, particularly in dynamic environments where a host is randomly joining to or leaving from the network. We will also study the implementation of the proposal in the elastic WLAN system, and evaluate the performance in various practical scenarios.

Acknowledgements

It is my great pleasure to express my heartiest thankfulness to those who gave me the valuable time and supported me in making this dissertation possible. I believe that you are the greatest blessing in my life. Thanks all of you to make my dream successful.

I owe my deepest sense of gratitude to my honorable supervisor, Professor Nobuo Funabiki for his excellent supervision, meaningful suggestions, persistent encouragements, and other fruitful help during each stage of my Ph.D. study. His thoughtful comments and guidance helped me to complete my research papers and present them in productive ways. Besides, he was always patient and helpful whenever his guidance and assistance were needed in both of my academic and daily life in Japan. I have really been lucky in working with a person like him. Needless to say, it would not have been possible to complete this thesis without his guidance and active support.

I am indebted to my Ph.D. co-supervisors, Professor Satoshi Denno and Professor Yasuyuki Nogami, for taking the valuable time to give me advice, guidance, insightful comments, and proof-reading my thesis.

I want to express my profound gratitude to Associate Professor Minoru Kuribayashi in Okayama University for his valuable discussions during my research. I would like to take this opportunity to thank and convey my respect to all of my course teachers during my Ph.D. study for sharing their great ideas and knowledge with me.

I would like to acknowledge the Ministry of Education, Culture, Sports, Science, and Technology of Japan (MEXT) for financially supporting my Ph.D. study, and the Begum Rokeya University, Rangpur, Bangladesh for giving me the study leave permission for this study.

I would like to thank for the fruitful discussions and cooperations with many people including Dr. Sritrusta Sukaridhoto, Dr. I-Wei Lai, Dr. Nobuya Ishihara, Dr. Md. Ezharul Islam, Dr. Md. Selim Al Mamun, Dr. Khin Khin Zaw, Dr. Kyaw Soe Lwin, Mr. Md. Manowarul Islam, Ms. Mousumi Saha, Mr. Kwenga Ismael Munene, and Mr. Rahardhita Widyatra Sudibyo. I would like to convey my respect to all the members of FUNABIKI Lab for their continued support during the period of this study. I would like to say special thanks to Dr. Kyaw Soe Lwin and Ms. Saha Mousumi for their great helps in this study.

I especially want to thank my beloved wife Mousumi Saha, who always comforts, consoles, and encourages me. Thank you for being with me in all the difficult time in Japan.

Finally, I am grateful to my family, my mom, dad, brothers, and all of my friends. For your unconditional loves, supports, patience, and confidence in me are the biggest rewards as well as the driving forces of my life.

List of Publications

Journal Paper

1. **Sumon Kumar Debnath**, Nobuo Funabiki, Mousumi Saha, Md. Selim Al Mamun, and Wen-Chung Kao, "MIMO host location optimization in active access-point configuration algorithm for elastic WLAN system," *Int. J. Space-Base. Sit. Comput.*, (IJSSC), vol. 8, no. 2, pp. 59-69, Aug. 2018.

International Conference Papers

2. Mousumi Saha, Nobuo Funabiki, **Sumon Kumar Debnath**, and Wen-Chung Kao, "A study of MIMO host location optimization in active access-point configuration algorithm for elastic WLAN system," *Proc. IEEE Int. Conf. Consum. Elect. Taiwan (ICCE-TW)*, pp. 275-276, May 2018.
3. **Sumon Kumar Debnath**, Mousumi Saha, Nobuo Funabiki, and Wen-Chung Kao, "A throughput estimation model for IEEE 802.11n MIMO link in wireless local-area networks," *Proc. 3rd Int. Conf. Comp. Commun. Syst. (ICCCS)*, pp. 327-331, April 2018.

Other Papers

4. **Sumon Kumar Debnath**, Nobuo Funabiki, Kyaw Soe Lwin, Kwenga Ismael Munene, and Mousumi Saha, "A modified throughput estimation model for concurrent communications in wireless network," *IEICE General Conf.*, pp. S-3-4, March 2018.
5. Mousumi Saha, Nobuo Funabiki, **Sumon Kumar Debnath**, and Kyaw Soe Lwin, "Modification of MIMO host location optimization for active access-point configuration algorithm in elastic WLAN system," *IEICE General Conf.*, pp. S-4-5, March 2018.
6. **Sumon Kumar Debnath**, Nobuo Funabiki, Kyaw Soe Lwin, and Md. Selim Al Mamun, "A study of throughput estimation model for IEEE 802.11n MIMO link in wireless local-area network," *IEICE Tech. Rep.*, vol. 117, no. 303, NS2017-114, pp. 17-22, Nov. 2017.
7. **Sumon Kumar Debnath**, Nobuo Funabiki, Kyaw Soe Lwin, Md. Selim Al Mamun, Munene Kwenga Ismael, and Md. Manowarul Islam, "Evaluations of throughput estimations in two network simulators for IEEE 802.11n wireless local-area networks," 2017 (68th) Chugoku-branch Joint Conv. Inst. Elec. Info. Eng., Oct. 2017.

8. **Sumon Kumar Debnath**, Nobuo Funabiki, Kyaw Soe Lwin, Md. Selim Al Mamun, R-hardhita Widyatra Sudibyo, and Samsul Huda, “Raspberry Pi configuration for access-point and its throughput measurements in IEEE802.11n wireless networks,” IEICE Tech. Rep., vol. 116, no.382, NS2016-137, pp. 101-106, Dec. 2016.

List of Figures

2.1	Components of IEEE 802.11 WLANs.	6
2.2	Operating modes of IEEE 802.11 networks.	7
2.3	Extended service set (ESS).	8
2.4	DCF basic access mechanism.	9
2.5	Throughput and collision rate of BEB algorithm.	10
2.6	Current and future WiFi Standards.	12
2.7	WiFi channels in 2.4 GHz band.	14
2.8	WiFi channels in 5 GHz band.	14
2.9	Comparison between SISO and 4×4 MIMO technology.	15
2.10	IEEE 802.11n channel bonding concept.	15
2.11	Link speed change for IEEE 802.11n 2×2 MIMO link.	16
2.12	Beamforming technology.	18
2.13	Comparison of modulation.	19
3.1	Elastic WLAN system topology.	24
4.1	Simple network configuration for measurement.	32
4.2	Three network fields.	34
4.3	Position of host in outdoor network field (<i>field#1</i>).	35
4.4	Measurement results for 2×2 MIMO and SISO links.	35
4.5	RSS and throughput estimation for 2×2 MIMO link in <i>field#1</i>	36
4.6	RSS and throughput estimation for SISO link in <i>field#1</i>	36
4.7	Throughput results in <i>field#1</i>	37
4.8	Throughput measurement results for 2×2 MIMO and SISO links in indoor fields.	38
4.9	Observed channel conditions at 2.4 GHz by Homedale network monitoring tool.	38
4.10	Sigmoid curve for 2×2 MIMO link in indoor <i>field#2</i>	39
4.11	Estimation results in indoor fields.	40
4.12	Throughput measurement results for different distances at corridor in <i>field#2</i>	41
4.13	Throughput estimation results at corridor in <i>field#2</i>	41
4.14	Throughput results in <i>field#1</i>	43
4.15	Throughput estimation results for Raspberry Pi AP (built-in NIC) in <i>field#2</i>	44
4.16	Performance results at different distances with different USB adapters.	45
4.17	Performance results at different hosts location with different USB wireless NIC adapters.	46
4.18	Experiment setup for two cases in <i>field#2</i>	47
4.19	Throughput results for one-room case in <i>field#2</i>	48
4.20	Throughput results for three-rooms case in <i>field#2</i>	48
4.21	Throughput estimation with reduction factor.	50

4.22	Host replicas for second model modification.	50
4.23	Evaluation results of the proposed model for SISO links in <i>field#2</i>	51
4.24	Evaluation results of proposed model for MIMO and SISO links in <i>field#2</i>	51
4.25	Evaluation results for proposed model for MIMO and SISO links in <i>field#3</i>	52
5.1	Throughput results with one MIMO and four SISO links.	55
6.1	Random topology for simulations.	62
6.2	Performance graphs for random topology.	63
6.3	Regular topology for simulations.	64
6.4	Performance graphs for regular topology.	65
6.5	Testbed scenario.	66

List of Tables

2.1	IEEE 802.11 Standards.	10
2.1	IEEE 802.11 Standards.	11
2.2	Characteristics of common IEEE 802.11 standards.	13
2.3	Specification of IEEE 802.11n.	13
2.4	Effects of channel width, MIMO links and guard interval on IEEE 802.11n's throughput.	16
2.5	Specification of IEEE 802.11ac.	17
2.6	Effects of channel bandwidth, spatial streams, and GI on IEEE 802.11ac's throughput.	18
4.1	Devices and software in measurements.	33
4.2	Parameter values with NEC AP for <i>field#1</i>	36
4.3	Throughput estimation error (Mbps) with NEC AP in <i>field#1</i>	37
4.4	Parameter values with NEC AP for <i>field#2</i> and <i>field#3</i>	38
4.5	Throughput estimation error (Mbps) with NEC AP in <i>field#2</i> and <i>field#3</i>	39
4.6	Parameter values with NEC AP for corridor in <i>field#2</i>	41
4.7	Throughput estimation error (Mbps) with NEC AP at corridor in <i>field#2</i>	42
4.8	Parameter values with Raspberry Pi AP for <i>field#1</i>	43
4.9	Throughput estimation error (Mbps) with Raspberry Pi in <i>field#1</i>	44
4.10	Parameter values with Raspberry Pi AP for <i>field#2</i>	44
4.11	Throughput estimation error (Mbps) with Raspberry Pi AP in indoor <i>field#2</i>	45
4.12	Throughput results (Mbps) for multiple links (only SISO) in <i>field#2</i>	49
4.13	Throughput results (Mbps) for multiple links (MIMO and SISO) in <i>field#2</i>	52
6.1	Parameter values for throughput estimation model.	61
6.2	PC environment for simulation.	61
6.3	Simulation results for the different number of MIMO hosts in random topology.	63
6.4	Simulation results for the different number of MIMO hosts in regular topology.	65
6.5	Throughput results.	66

Contents

Abstract	i
Acknowledgements	iii
List of Publications	v
List of Figures	viii
List of Tables	ix
1 Introduction	1
1.1 Background	1
1.2 Contributions	3
1.3 Related Works	3
1.4 Thesis Outline	4
2 IEEE 802.11 Wireless Network Technologies	5
2.1 802.11 WLAN Overview	5
2.1.1 IEEE 802.11 WLAN Components	6
2.1.2 Operating Modes for IEEE 802.11 WLAN	6
2.1.3 Channel Access Modes in IEEE 802.11 MAC Standard	7
2.1.4 DCF Operations	8
2.1.4.1 DCF Access Mechanism	8
2.1.4.2 Binary Exponential Backoff Mechanism	9
2.2 IEEE 802.11 Standards for WLAN	10
2.3 IEEE 802.11n Protocol	12
2.3.1 Link Speed Change Feature of IEEE 802.11n MIMO Links	16
2.4 IEEE 802.11ac Protocol	17
2.5 Commercial and Software APs	19
2.6 Summary	20
3 Review of Previous Studies	21
3.1 Throughput Estimation Model for IEEE 802.11n Link	21
3.1.1 Overview	21
3.1.2 Receiving Signal Strength Estimation	21
3.1.2.1 Log Distance Path Loss Model	21
3.1.2.2 Multipath Effect	22
3.1.3 Throughput Conversion by Sigmoid Function	22

3.1.4	Parameter Optimization Tool	22
3.1.5	Procedure for Throughput Estimation	23
3.2	Elastic WLAN System	23
3.2.1	Overview	23
3.2.2	Implementation	23
3.3	Active AP Configuration Algorithm	23
3.3.1	Problem Formulation	24
3.3.2	Algorithm Procedure	26
3.3.2.1	Active AP and Associated Host Selection Phase	26
3.3.2.2	Channel Assignment Phase	28
3.3.2.3	Channel Load Averaging Phase	29
3.4	Summary	30
4	Throughput Measurements and Estimation Models under Various Conditions	31
4.1	Introduction	31
4.2	Experiment Setups	32
4.2.1	Devices and Software Tools	32
4.2.2	Network Fields	33
4.3	Results for Commercial AP	34
4.3.1	Results in Outdoor Environment	34
4.3.2	Results in Indoor Environment	37
4.3.2.1	Results at Different Hosts Location	37
4.3.2.2	Results at Different Distances in Corridor	40
4.4	Results for Raspberry Pi AP	42
4.4.1	Configuration of Raspberry Pi for Software AP	42
4.4.2	Results in Outdoor Environments	43
4.4.3	Results in Indoor Environments	44
4.4.4	Comparisons between Different USB Adapters	45
4.5	Throughput Estimation for Concurrent Communication	46
4.5.1	Experiment Setup	47
4.5.2	Measurement Results	47
4.5.2.1	Measurement Results for one-room case	48
4.5.2.2	Measurement Results for three rooms case	48
4.5.3	Model Modifications	49
4.5.4	Evaluation Results	51
4.6	Summary	52
5	Proposal of MIMO Host Location Optimization Approach	54
5.1	Introduction	54
5.2	Motivation of MIMO host location optimization	55
5.3	Proposal of MIMO host location optimization algorithm	55
5.3.1	Problem Formulation	56
5.3.2	Algorithm Procedure	57
5.4	Summary	58

6	Evaluation of MIMO Host Location Optimization Approach	60
6.1	WIMNET Simulator	60
6.2	Network Environments	60
6.3	Model Parameters	61
6.4	Hardware and Software	61
6.5	Evaluation in Random Topology	62
6.5.1	Network Topology	62
6.5.2	Simulation Results	62
6.6	Evaluation in Regular Topology	64
6.6.1	Network Topology	64
6.6.2	Simulation Results	65
6.7	Testbed Experiment Results	66
6.8	Summary	66
7	Conclusion	67
	References	69

Chapter 1

Introduction

1.1 Background

Recently, the Internet has played an essential role in making our daily life easy and convenient. People can easily communicate with each other, and access various information and services electronically over the Internet. This massive progress of the Internet utilization in life causes huge demands of high speed, cost-effective and flexible Internet access services at various places around the world [1].

A common solution is the use of the IEEE 802.11n *wireless local-area network (WLAN)*. In WLAN, a variety of *access points (APs)*, mobile terminals, and desktop/laptop personal computers (PCs) are available with the strength of higher data rates and ranges, and the backward compatibility to the earlier IEEE 802.11a/b/g protocols [2]. IEEE 802.11n adopts several new technologies such as the *Multiple-Input Multiple-Output (MIMO)*, the *channel bonding*, the *frame aggregation*, and the *block acknowledgment (ACK)* mechanism to meet the demands for faster data transmissions [3].

The *Single-Input Single-Output (SISO)* link with the single antenna can provide the physical data rate up to 150Mbps (standard value) with the 40MHz bonded channel and the 400ns *guard interval (GI)* mode. However, the data rate of the SISO link can be reduced by multi-path, fading, and interferences [4]. For the higher transmission capacity and the better link reliability, the MIMO link is necessary. Using MIMO, the number of simultaneous data streams is increased by the number of antennas at the transmitter and the receiver [5]. For example, the IEEE 802.11n protocols can support the physical data rate up to 600Mbps with the 4×4 MIMO technology, the 40MHz channel, and the 400ns *GI*. More antennas can increase spatial diversity and spatial multiplexing that provide further gains in the channel robustness and the throughput in the MIMO technology [6].

A host in WLAN indicates a device that has the capability of connecting to the Internet through the WLAN interface. It includes a personal computer (desktop/laptop PC), a smartphone, and a tablet. PCs, main hosts in WLAN, are usually used at fixed positions in an *indoor network environment* that may consist of several rooms for laboratories, classrooms, or offices in a university or company. In such an environment, users normally access the Internet while sitting on chairs and putting their PCs on tables, because PCs are much larger and heavier than smart phones, and often require the use of both hands. As a result, the mobility of WLAN users is much lower than that of the cellular system users. Therefore, the possible locations of the hosts can be determined by the locations of desks and chairs, which can be fixed.

Currently, a lot of organizations or educational institutions install WLANs by using commercial

dedicated APs from certified vendors. These APs are often installed in the network field in a random way, which leads to lower throughput performances arising from interferences of wireless signals among different APs and hosts [7]. Thus, the configuration of the active APs should be optimized according to the traffic demands and the network situation in the field by deactivating redundant APs. Actually, the number of communicating hosts fluctuates with time of a day or a week. For example, in a university, a great number of students access to the network in the afternoon on weekdays, while much fewer students do so in the morning/evening and on weekends. Besides, the state of a WLAN can be affected by power shortages, device failures, bandwidth controls by authorities, or weather conditions [8]. The network configuration of WLAN should be properly managed by adapting to these changes.

To offer the solutions to the above-mentioned problems, we have studied the *elastic WLAN system* and the *active AP configuration algorithm* [9–12], which dynamically optimize the number of active APs according to traffic demands and network situations. Three types of APs, namely, a *dedicated AP (DAP)*, a *virtual AP (VAP)*, and a *mobile AP (MAP)* are considered in them. A *DAP* represents a commercial AP, a *VAP* does a host PC of a user in the network that installs the software of AP functions [13], and a *MAP* does a *mobile router*. Unfortunately, with the current active AP configuration algorithm, it is assumed that each AP and host only uses the slower SISO link for wireless communications, although MIMO technology has become available as the faster communication technology among commercial APs and PC models.

At present, nearly all the commercial APs have adopted the MIMO technology, while only the subset of hosts may use MIMO, because PCs with MIMO or *MIMO hosts* are more expensive than PCs with SISO or *SISO hosts*. Then, the proper locations of the limited MIMO hosts in the network field become critical to improve the communication performance by maximizing the potential ability of MIMO communications.

As the practical application of this proposal, the network manager controls the locations of the MIMO hosts by following the algorithm output. For example, in a university, a computer exerciser room and a laboratory can be this case. If the network manager cannot control them, still, he/she can encourage the MIMO host users to move to the locations specified by the algorithm output by showing the instructions or giving some incentives such as discounts at use of WLANs.

For the MIMO host location optimization, the accurate throughput estimation of a MIMO/SISO link is important. During the optimization process, the throughput must be estimated accurately when a host is located at different locations in the network field. By repeating the throughput estimation, the design of a WLAN system can be improved with low costs before its actual deployment.

In an indoor environment, the accurate estimation of throughput of a wireless link is challenging [14]. The transmission path between an AP and a host in indoors becomes much more complicated from the outdoors, due to the signal attenuations by different types of walls, floors, and other obstacles [15, 16], in addition to multipath effects. The throughput estimation needs proper considerations of floor plans, construction materials, types and thickness of walls, and multi-path effects. Network designers need to carefully tune these parameter values for the accurate throughput estimation of IEEE 802.11n links in a real environment.

Furthermore, the *concurrent communication* of multiple hosts with a single AP is common practically. It offers different throughput features from the *single host communication*, due to the increasing collision rate as the number of concurrent communicating hosts [17]. Besides, the AP receives the packet with the stronger signal successfully with the higher probability, when the *signal-to-interference-plus-noise-ratio (SINR)* is above the certain threshold [18–20]. As a result, hosts with the strong RSS may dominate the channel for long time, which causes unfairness

among the links. These effects must be considered in the throughput estimation model for accurate throughput estimation of MIMO/SISO links in practical network scenarios.

1.2 Contributions

In this thesis, first, we study the *throughput estimation model* under various conditions [21–24]. Here, both cases are considered: 1) a single host communication with an AP at a time, and 2) concurrent communications of multiple hosts with a single AP at a time. First, we present the measurement results of WLAN in both indoor and outdoor environments. We employ PCs with IEEE 802.11n 2×2 MIMO and 1×1 SISO links for user hosts, and commercial dedicated APs, and software APs using Raspberry Pi for APs.

We analyze the relationship in the *transmission control protocol (TCP)* throughput, the *received signal strength (RSS)*, and the link distance. The measurement results show that the throughput and RSS are greatly affected by the type of the AP or the PC, the link distance between the AP and the host, and the network environment. Then, we find the parameter values for the throughput estimation model by applying the parameter optimization tool to the measurement data [25], and verify the throughput estimation accuracy of MIMO/SISO links with the measurement results.

We also propose two modifications of the previous throughput estimation model, particularly to consider the concurrent communication of multiple hosts with one AP in indoor environments [24, 26]. The comparisons of the estimated throughput and the measured one support the correctness of our proposal.

Next, we propose the *MIMO host location optimization* approach as an extension of the active AP configuration algorithm in the elastic WLAN system [27]. This approach repeats exchanging the location of a randomly selected MIMO host with that of a randomly selected SISO host, if the result can satisfy the constraints of the network and improve the total throughput performance by the given times.

The effectiveness of the proposed MIMO host location optimization approach is verified through simulations in two network topologies using the *WIMNET simulator* [28]. The improvement of throughput performance is confirmed by comparing the outcomes before and after applying for the proposed extension. The CPU time to complete the proposed algorithm is also evaluated.

1.3 Related Works

To optimize the performance of WLAN, the link speed or throughput of a wireless link between an AP and a host in the WLAN should be estimated accurately. Several studies have been reported for designing, modelling, analysis, measurements, and estimations of the throughput performance of the WLAN system.

In [29], Dama et al. measured and analysed the operational throughput performance of a commercial IEEE 802.11n MIMO 2×3 dual-band system at $2.4GHz$ and $5GHz$ in indoor environments with both *Line of Sight (LoS)* and *Non Line of Sight (NLoS)* scenarios.

In [30], Jansons et al. presented the performance analysis of the IEEE 802.11n protocol with respect to the link distance, the throughput, and the signal to noise ratio (SNR).

In [31], Chew et al. evaluated the link speed change feature by changing the distance between an AP and a host using commercial WiFi devices, and introduced a link speed estimation equation from the distance. Unfortunately, in the real network field, the link distance cannot be obtained in real time.

In [32], Choi et al. developed a theoretical throughput estimation method for the IEEE 802.11 WLAN to estimate the throughput that each node would achieve in WLAN where nodes may have heterogeneous traffic demands, data transmission rates, and packet sizes. They evaluated the method through extensive packet level simulations using the network simulator *ns-3*.

In [33], Vanhatupa et al. evaluated a throughput estimation model and an optimization algorithm for the frequency planning of the WLAN system. The result of the throughput estimation model is used as the input to the optimization algorithm to maximize the multi-cell WLAN throughput.

In [34], Bruno et al. measured and analysed the throughput of IEEE 802.11 WLAN, and presented a Markov chain based performance model. This model does not support IEEE 802.11n protocol.

In [18], Hosseinabadi et al. presented the design and the performance evaluation of the concurrent MAC mechanism that uses the opportunistic overhearing to schedule the network nodes for concurrent transmissions in dense WLANs. The concurrent MAC mechanism can increase concurrent transmissions and aggregate the throughput compared to IEEE 802.11 DCF by identifying the successful concurrent transmissions in dense WLANs. According to [35], concurrent transmissions in low-power wireless networks are almost possible through the appropriate selections of transmission powers and channels.

Based upon our surveys, the same topic of the MIMO host location optimization in IEEE 802.11 WLAN as in this thesis has not been reported. On the other hand, a variety of research works have been reported on the location optimization of APs in WLAN [36–40].

1.4 Thesis Outline

The remaining part of this thesis is organized as follows.

In Chapter 2, we briefly review related IEEE 802.11 wireless network technologies to this study, including the IEEE 802.11n/ac protocols, commercial APs, and software APs.

In Chapter 3, we provide the review of our previous related studies.

In Chapter 4, we present the throughput measurement results for IEEE 802.11n links under various conditions in indoor and outdoor environments, and extend the throughput estimation model by considering the concurrent communication of multiple hosts with a single AP.

In Chapter 5, we present the MIMO host location optimization approach by considering the effect in concurrent communication as an extension of the active AP configuration algorithm for elastic WLAN system for improving the throughput performance.

In Chapter 6, we evaluate the MIMO host location optimization approach through extensive simulations in two network instances and testbed experiments.

Finally, in Chapter 7, we conclude this thesis with some future works.

Chapter 2

IEEE 802.11 Wireless Network Technologies

In this chapter, we overview related WLAN technologies as backgrounds of this thesis. First, we review *IEEE 802.11 protocols*. Then, we discuss the *IEEE 802.11n protocol*, especially, the key technologies, the link speed change features with MIMO and SISO links that are used in the thesis. Then, we briefly introduce the *IEEE 802.11ac protocol*. Finally, we describe the commercial AP and the software AP technology.

2.1 802.11 WLAN Overview

IEEE 802.11 standards determine *physical (PHY)* and *media access control (MAC)* layer specifications for implementing high-speed *wireless local area network (WLAN)* technologies. WLAN is an extension to a wired LAN that enables wireless connectivity for the user mobility and supports flexibility in data communications [41]. It can reduce the cabling costs in the home or office environments by transmitting and receiving data over the air using *radio frequency (RF)* technology. IEEE 802.11 provides the set of standards for WLAN.

WLAN offers several benefits over the traditional wired networks. Specific benefits are included in the following [41]:

- *User mobility:*
In wired networks, users need to use wired lines to stay connected to the network. On the other hand, WLAN allows user mobility within the coverage area of the network.
- *Easy and rapid deployment:*
WLAN system can exclude the requirement of network cables between hosts and connection hubs or APs. Thus, the installation of WLAN can be much easier and quicker than wired LAN.
- *Cost:*
The initial installation cost can be higher than the wired LAN, but the life-cycle costs can be significantly lower. In a dynamic environment requiring frequent movements or reconfigurations of the network, WLAN can provide the long-term cost profit.
- *Increased flexibility:*
The network coverage area by WLAN can be easily expanded because the network medium is already everywhere.

- *Scalability:*

Depending on applications, WLAN can be configured in a variety of topologies. They can support both peer-to-peer networks suitable for a small number of users and full infrastructure networks of thousands of users.

2.1.1 IEEE 802.11 WLAN Components

IEEE 802.11 WLAN consists of four primary components as shown in Figure 2.1 [41]:

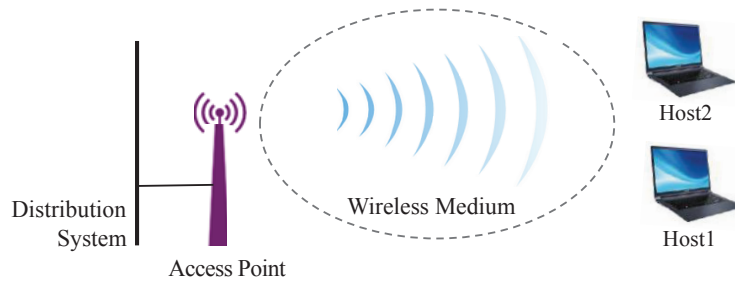


Figure 2.1: Components of IEEE 802.11 WLANs.

- *Hosts:*

WLAN transfers data between *hosts*. A host in WLAN indicates an electronic device such as a desktop/laptop PC, a smartphone, or a Personal Digital Assistants (PDA) that has the capability to access the network over the wireless network interface card (NIC).

- *Access points (APs):*

An AP acts as the main radio transceiver or a generic base station for a WLAN that plays the similar role as a hub/switch in wired Ethernet LAN. It also performs the bridging function between the wireless and the wired networks with some other tasks.

- *Wireless medium:*

The IEEE 802.11 standard uses the wireless medium to flow the information from one host to another host in a network.

- *Distribution system:*

When several APs are connected together to form a large coverage area, they must communicate with each other to track the movements of the hosts. The distribution system is the logical component of WLAN which serves as the backbone connections among APs. It is often called as the *backbone network* used to relay frames between APs. In most cases, *Ethernet* is commonly used as the backbone network technology.

2.1.2 Operating Modes for IEEE 802.11 WLAN

The elementary unit of IEEE 802.11WLAN is simply a set of hosts that can communicate with each other known as the *basic service set (BSS)*. Based on the types of BSS, the IEEE 802.11 supports two operating modes as illustrated in Figure 2.2.

- *Independent mode:*

In this mode, a collection of hosts can send frames directly to each other without an AP. It is also called as an *independent BSS (IBSS) mode* as shown in Figure 2.2(a). This *ad hoc network* is rarely used for permanent networks due to the lack of required performances and security issues.

- *Infrastructure mode:*

In this mode, the hosts exchange their information through an AP as shown in Figure 2.2(b). A single AP acts as the main controller to all the hosts within its BSS, known as *infrastructure BSS*. In this mode, a host must be associated with an AP to obtain network services [42].

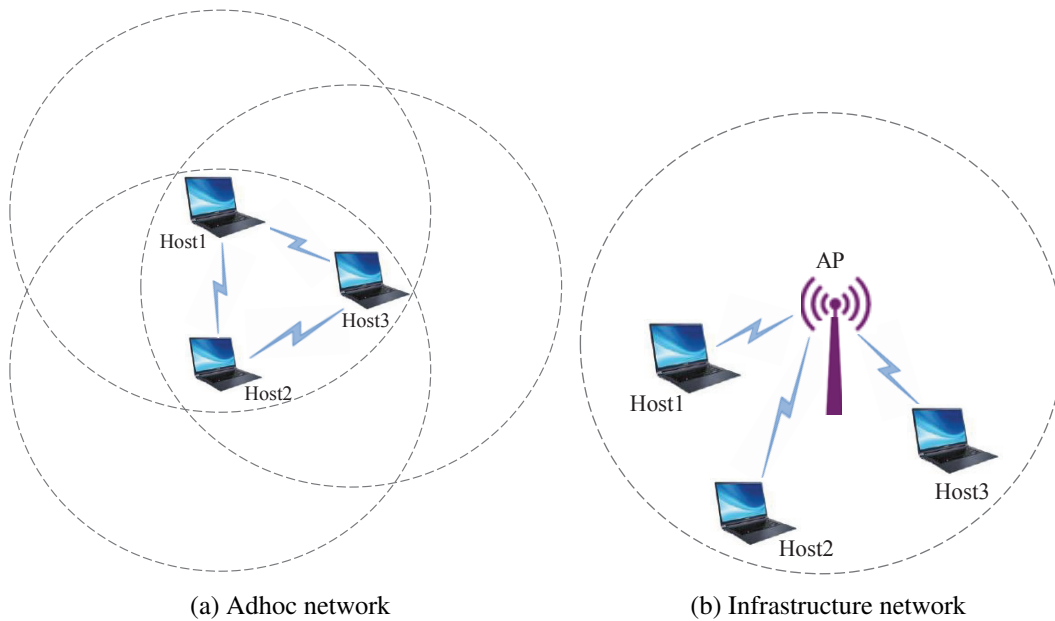


Figure 2.2: Operating modes of IEEE 802.11 networks.

In addition, multiple BSSes can be connected together with a backbone network to form *extended service set (ESS)* as shown in Figure 2.3.

It can form a large size WLAN. Each AP in an ESS is given an ID called the *service set identifier (SSID)*, which serves as a “network name” for the users. Hosts within the same ESS can communicate with each other, even if they are in different basic service areas.

2.1.3 Channel Access Modes in IEEE 802.11 MAC Standard

The IEEE 802.11 MAC standard includes two basic channel access modes: *distributed coordination function (DCF)* and *point coordination function (PCF)*. DCF is the contention-based fundamental MAC mechanism of the IEEE 802.11 WLAN which employs the *CSMA/CA protocol*, and an ordinary *binary exponential backoff (BEB)* algorithm. For contention-free services, PCF is an optionally used. PCF is the polling based protocol limited to the infrastructure based network.

DCF is broadly implemented in most commercial products due to its simplicity and robustness. Therefore, most researchers have given their attention on DCF. Two types of *carrier sensing (CS)* is used in IEEE 802.11 to check if the medium is idle or not. They are the physical carrier sensing

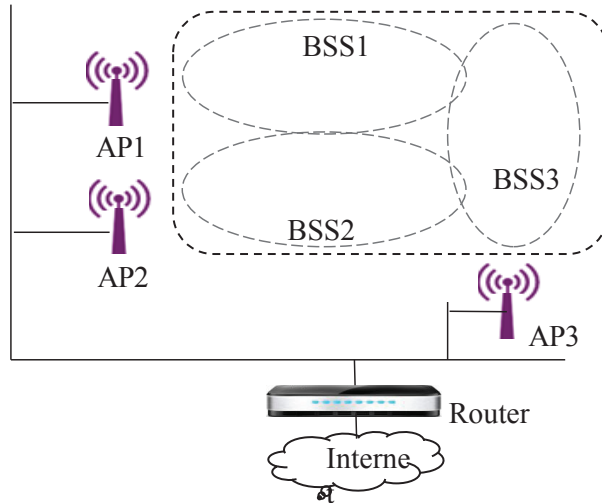


Figure 2.3: Extended service set (ESS).

at the physical layer and the virtual carrier sensing at the MAC layer. The virtual carrier sensing is provided by *Network Allocation Vector (NAV)*. The station set NAV to the time where they need to reserve the medium for its data transmissions [41].

In the IEEE 802.11 MAC protocol, the *inter-frame spacing (IFS)* is used for coordinating the access to the wireless medium. Actually, three basic inter-frame spaces are used: *short IFS (SIFS)*, *point coordination function IFS (PIFS)*, and *distributed coordination function IFS (DIFS)*. The time duration of them is: $SIFS < PIFS < DIFS$.

2.1.4 DCF Operations

DCF has two basic transmission modes to enable the random access to the wireless channel. One is the basic access method using two-way handshakes (DATA + ACK), and another one is the four-way handshakes optionally used by exchanging RTS/CTS messages to reserve the channel before each data transmission.

2.1.4.1 DCF Access Mechanism

In the DCF mechanism, a station wishing to transmit packets first listens to the channel status for more than the DIFS interval. If the channel remains free, this station (sender) sends the packet to the destination (receiver) immediately. The receiver responds to the acknowledgment (ACK) frame after the SIFS interval. If the channel is busy or the idle time is less than DIFS, the sender defers the transmission and uses the binary exponential backoff (BEB) mechanism to avoid the collisions among the contending nodes while providing their fairness. The length of the random backoff time is determined by:

$$T_{bo} = rand(CW) \times T_{slot} \quad (2.1)$$

where T_{bo} represents the backoff period, T_{slot} does the time slot, and CW is the contention window or backoff window in terms of time slots. The contention window is divided into time slots whose length depends on the medium. Stations are activated at the beginning of each slot [41]. The DCF basic access mechanism is shown in Figure 2.4.

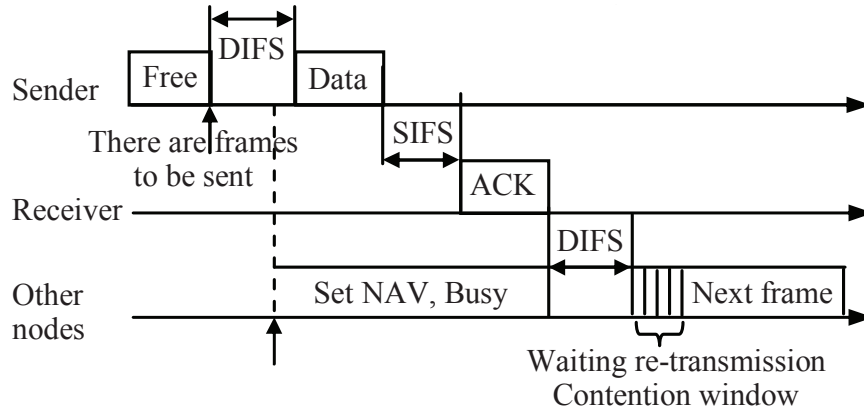


Figure 2.4: DCF basic access mechanism.

2.1.4.2 Binary Exponential Backoff Mechanism

The binary exponential backoff (BEB) algorithm is used in the IEEE 802.11 DCF to schedule retransmissions after collisions in order to avoid collisions again. In the DCF, any station must carry out carrier sensing at the channel for the interval larger than DIFS before attempting any data transmission. If the channel is found busy, the station defers its transmission until the medium is idle for DIFS. Then, the station generates a backoff time with a random value that is uniformly selected from the range $[0, CW - 1]$, where CW is the current window size. At the first transmission attempt, CW is initially set to CW_{min} . The backoff timer is decreased each time when the channel is sensed idle, or is frozen when the channel seems busy due to other nodes transmissions, and is restarted again when the channel is sensed free again for more than DIFS. When the backoff timer reaches zero, the station initiates its transmission of the next time slot. If the packet is received successfully, the receiver sends back ACK after the SIFS interval and resets its CW to CW_{min} .

If the sender fails to get ACK within the specified period, the retransmission will be scheduled. It doubles the CW size, under the maximum value of $CW_{max} = 2^m \times CW_{min}$, where m is the maximum backoff stage. Then, it chooses a new random backoff timer, and starts the above process again. When the transmission of a packet fails for a maximum number of times, this packet is dropped.

It is clear that the size of CW increases rapidly with the number of retransmission attempts, and reduces the collision probability. The main reason for the low throughput performance and the poor channel utilization of the IEEE 802.11 MAC protocol is the retransmission. The MAC layer congestion occurs due to the high packet error rate, the limited bandwidth, the large contention, and the long backoff time. When some stations suffer from higher packet loss rates due to higher errors, they will turn to the backoff state more frequently than stations with low error rates, which leads to the backoff window larger for them. On the other hands, stations with lower error rates can get more transmission chances, causing the unfairness problem in WLAN [43].

The BEB mechanism performs well with a small number of active stations. However, when the number of stations increases beyond a certain limit, its throughput performance decreases desperately as shown in Figure 2.5. In this case, the collision rate increases with the number of active stations, and the throughput drops significantly [17].

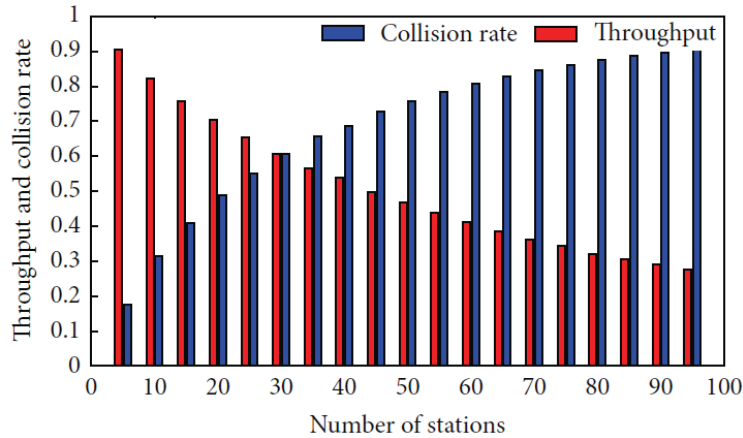


Figure 2.5: Throughput and collision rate of BEB algorithm.

2.2 IEEE 802.11 Standards for WLAN

The IEEE 802.11 working group improves the existing PHY and MAC layer specifications to realize WLAN at the 2.4-2.5 GHz, 3.6 GHz and 5.725-5.825 GHz unlicensed ISM (Industrial, Scientific and Medical) frequency bands defined by the ITU-R. In this working group, several types of IEEE Standard Association Standards are available, where each of them comes with a letter suffix, covers from wireless standards, to standards for security aspects, Quality of Service (QoS) and others, shown in Table 2.2 [42, 44–48].

Table 2.1: IEEE 802.11 Standards.

Standard	Purpose
802.11a	Wireless network bearer operating in the 5 GHz ISM band, data rate up to $54Mbps$
802.11b	Operate in the 2.4 GHz ISM band, data rates up to $11Mbps$
802.11c	Covers bridge operation that links to LANs with a similar or identical MAC protocol
802.11d	Support for additional regulatory differences in various countries
802.11e	QoS and prioritization, an enhancement to the 802.11a and 802.11b WLAN specifications
802.11f	Inter-Access Point Protocol for handover, this standard was withdrawn
802.11g	Operate in 2.4 GHz ISM band, data rates up to $54Mbps$
802.11h	Dynamic Frequency Selection (DFS) and Transmit Power Control (TPC)
802.11i	Authentication and encryption
802.11j	Standard of WLAN operation in the 4.9 to 5 GHz band to conform to the Japan's rules
802.11k	Measurement reporting and management of the air interface between several APs
802.11l	Reserved standard, to avoid confusion
802.11m	Provides a unified view of the 802.11 base standard through continuous monitoring, management and maintenance

Table 2.1: IEEE 802.11 Standards.

Standard	Purpose
802.11n	Operate in the 2.4 and 5 GHz ISM bands, data rates up to 600Mbps
802.11o	Reserved standard, to avoid confusion
802.11p	To provide for wireless access in vehicular environments (WAVE)
802.11r	Fast BSS Transition, supports VoWiFi handoff between access points to enable VoIP roaming on a WiFi network with 802.1X authentication
802.11s	Wireless mesh networking
802.11t	Wireless Performance Prediction (WPP), this standard was cancelled
802.11u	Improvements related to "hotspots" and 3rd party authorization of clients
802.11v	To enable configuring clients while they are connected to the network
802.11w	Protected Management Frames
802.11x	Reserved standard, to avoid confusion
802.11y	Introduction of the new frequency band, 3.65-3.7GHz in US besides 2.4 and 5 GHz
802.11z	Extensions for Direct Link Setup (DLS)
802.11aa	Specifies enhancements to the IEEE 802.11 MAC for robust audio video (AV) streaming
802.11ac	Wireless network bearer operating below 6 GHz to provide data rates of at least 1Gbps for multi-station operation and 500Mbps on a single link
802.11ad	Wireless Gigabit Alliance (WiGig), providing very high throughput at frequencies up to 60GHz
802.11ae	Prioritization of management frames
802.11af	WiFi in TV spectrum white spaces (often called White-Fi)
802.11ah	WiFi uses unlicensed spectrum below 1GHz, smart metering
802.11ai	Fast initial link setup (FILS)
802.11aj	Operation in the Chinese Milli-Meter Wave (CMMW) frequency bands
802.11ak	General links
802.11aq	Pre-association discovery
802.11ax	High efficiency WLAN, providing 4x the throughput of 802.11ac
802.11ay	Enhancements for Ultra High Throughput in and around the 60GHz Band
802.11az	Next generation positioning
802.11mc	Maintenance of the IEEE 802.11m standard

Figure 2.6 shows the current and future WiFi standards. Among these standards, the common and popular ones are IEEE 802.11a, 11b, 11g, 11n, and 11ac. For the physical layer, the 11a/n/ac use *Orthogonal Frequency Division Multiplexing (OFDM)* modulation scheme while the 11b uses the *Direct Sequence Spread Spectrum (DSSS)* technology. 11g supports both technologies. Table 2.2 summarizes the features of these common WiFi standards [41, 49, 50].

- *IEEE 802.11b*: IEEE 802.11b operates at 2.4 GHz band with the maximum data rate up to 11 Mbps. 802.11b is considered to be a robust system and has a capacity to compensate the same IEEE 802.11 protocols. Because of the interoperability feature between products from different vendors, this standard has not only boosted the manufacturing of the products but

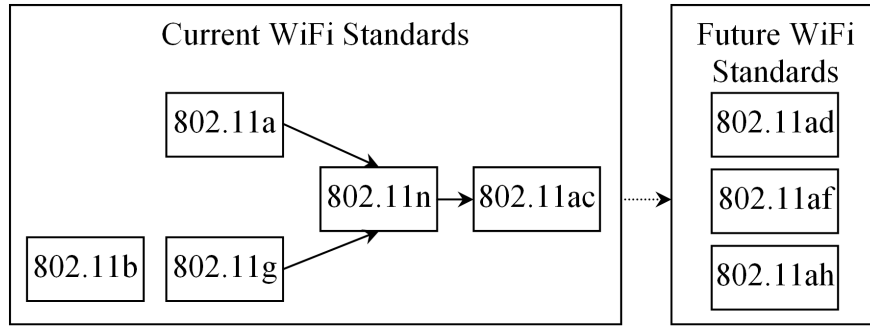


Figure 2.6: Current and future WiFi Standards.

also motivated the competitions between WLAN vendors. The limitation of this standard is the interference among the products using *industrial, scientific and medical* (ISM) band that uses the same 2.4 GHz band of frequency [51, 52].

- *IEEE 802.11a*: IEEE 802.11a operates at 5 GHz ISM band. It adopts an orthogonal frequency division multiplexing (OFDM) coding scheme that offers a high data rate up to 6, 12, 24, 54 Mbps, and sometimes beyond this speed in comparison to 802.11b. Two main limitations of 802.11a are the compatibility issue of the 802.11a products with 802.11b products and the unavailability of 5 GHz band with free of cost for all the countries in the world [51, 52].
- *IEEE 802.11g*: IEEE suggested 802.11g standard over 802.11a to improve the 2.4 GHz 802.11b technology. 802.11g introduces two different modulation techniques including the *packet binary convolution code (PBCC)* that supports data rate up to 33Mbps and the *orthogonal frequency division multiplexing (OFDM)* that supports up to 54Mbps data rate. Compatibility issues are also resolved in 802.11g products with 802.11b products [51, 52].
- *IEEE 802.11n*: The primary purpose of initiating the 802.11n standard to improve the usable range and data rate up to 600Mbps. 802.11n supports both of 2.4 GHz and 5 GHz ISM band *unlicensed national information infrastructure* (UNII) band, and is backward compatible with earlier standards. It introduces new technology features including the use of channel bonding and multiple antennas to get the better reception of the RF signals to enhance the throughput and coverage range [51, 53].
- *IEEE 802.11ac*: The aim of the 802.11ac standard to improve individual link performance and total network throughput of more than 1Gbps. Many of the specifications like static and dynamic channel bonding and simultaneous data streams of 802.11n have been kept and further enhanced for 802.11ac to reach the gigabit transmission rate. It supports static and dynamic channel bonding up to 160MHz and *Multi-User Multiple-Input-Multiple-Output (MU-MIMO)*. 802.11ac operates only on the 5 GHz band [54–56].

2.3 IEEE 802.11n Protocol

In this section, we review the IEEE 802.11n protocol that we have considered in this thesis. 11n was actually developed with the aim of increasing the PHY and MAC layer throughput over its

Table 2.2: Characteristics of common IEEE 802.11 standards.

	IEEE 802.11b	IEEE 802.11a	IEEE 802.11g	IEEE 802.11n	IEEE 802.11ac
Release	Sep 1999	Sep 1999	Jun 2003	Oct 2009	Dec 2013
Frequency Band	2.4 GHz	5 GHz	2.4 GHz	2.4/5 GHz	5 GHz
Max. Data Rate	11 Mbps	54 Mbps	54 Mbps	600 Mbps	1300 Mbps
Modulation	CCK ¹ modulated with PSK	OFDM	DSSS ² , CCK, OFDM	OFDM	OFDM
Channel Width	20 MHz	20 MHz	20 MHz	20/40 MHz	20/40/80/160 MHz
# of Antennas	1	1	1	4	8
security	Medium	Medium	Medium	High	High

¹ CCK: Complementary Code Keying

² DSSS: Direct Sequence Spread Spectrum

previous standards (11a, 11b, and 11g). The standard uses the multiple antennas technology, channel bonding, frame aggregation, and security improvements mechanism to improve the throughput [53]. Table 2.3 shows a brief summary of this standard.

Table 2.3: Specification of IEEE 802.11n.

Specification	IEEE 802.11n	
Frequency Band	2.4 GHz	5 GHz
Available Channel	13 ch	19 ch
Simultaneous Uninterrupted Channel	2 ch	9 ch
Max. Throughput	600Mbps	
Max. # of Spatial Streams	4	
Max. Modulation Types	64 QAM	
Max. Coding Rate	5/6	
Max. Channel Width	40 MHz	
Guard Interval	800 ns	400 ns
Release Date	September 2009	

IEEE 802.11n protocol can be operated in two unlicensed frequency bands namely the 2.4 GHz band or the 5 GHz band. In the 2.4 GHz band, 13 channels are available where the only limited number of them are non-overlapping. It is only four in 20MHz bandwidth. For 40MHz bandwidth channel, which is commonly used in IEEE 802.11n protocol, it is reduced by two (channel 3 and channel 11). This means that, the wider bandwidth can increase the physical data rate but it also reduces the number of available non-interfered channels. Figure 2.7 [47] shows the 20MHz WiFi channels in the 2.4 GHz band.

Although the 2.4 GHz band is very popular as inherited from IEEE 802.11g standard, it becomes crowded with a lot of WiFi signals. As a result, these devices using adjacent channels will

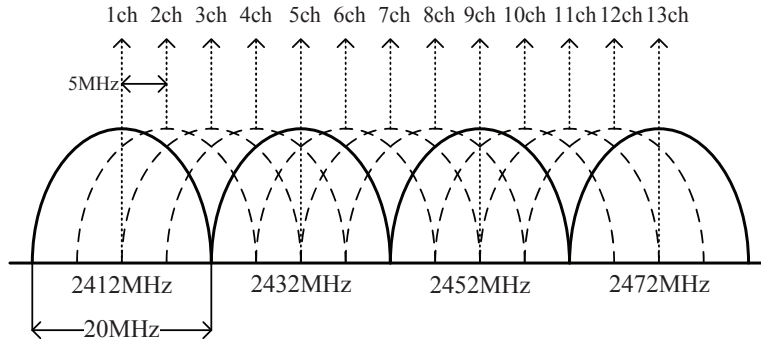


Figure 2.7: WiFi channels in 2.4 GHz band.

suffer from interferences and degrade the throughput performance [48]. Therefore, recently users start using the 5 GHz band.

In the 5 GHz band of IEEE 802.11n protocol, it has 19 uninterrupted channels available in the 20MHz bandwidth. In the 40MHz bandwidth, which doubles the channel width from the 20MHz, there are 9 channels. For the 80MHz bandwidth, there are four of them. Figure 2.8 [57] shows these WiFi channels for the IEEE 802.11n 5 GHz band.

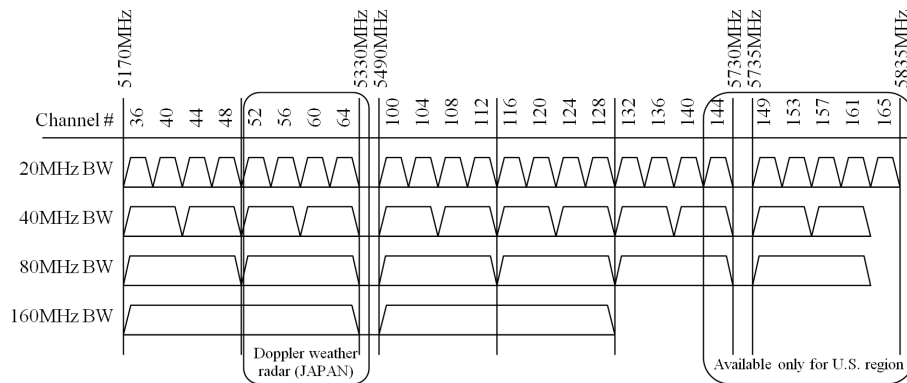


Figure 2.8: WiFi channels in 5 GHz band.

IEEE 802.11n protocol incorporates several new technologies to boost up its performance.

- **MIMO:**

In MIMO, the throughput can be linearly increased to the number of transmitting (T_X) and receiving (R_X) antennas up to four times, without the additional bandwidth or transmission power. The coverage area can be enhanced over the single antenna technology in *SISO*. The multiple antenna configurations in *MIMO* can overcome the detrimental effects of multi-path and fading, trying to achieve high data throughput in limited bandwidth channels. For example, in the 4×4 MIMO, four independent data streams can be multiplexed and transmitted simultaneously with the *spatial division multiplexing (SDM)*, to speed up the transmission capacity by quadruple as shown in Figure 2.9.

When the *space-time block coding (STBC)* is adopted in the 4×4 MIMO link, the sender can transmit four copies of the data stream over four antennas to improve the reliability and the effective range of data transmissions.

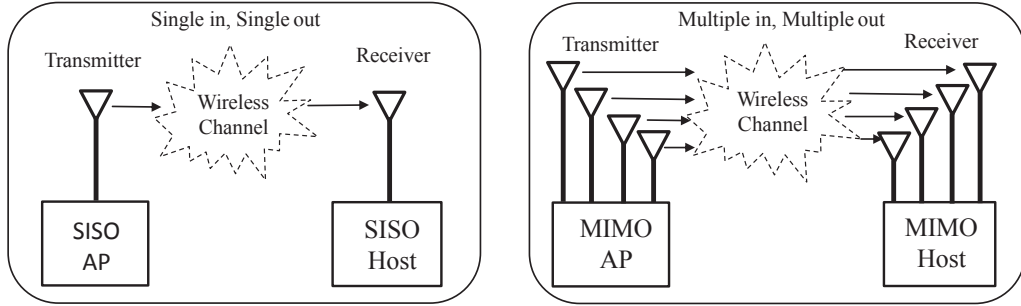


Figure 2.9: Comparison between SISO and 4×4 MIMO technology.

- *Channel Bonding:*

In the channel bonding, each channel can operate with the 40MHz bandwidth by using two 20MHz adjacent channels together to double its physical data rate [58] as shown in Figure 2.10. However, the usage of the channel bonding will reduce the available non-interfered channels for other devices as there are only two non-interfered bonded channels available for IEEE 802.11n protocol at 2.4 GHz band.

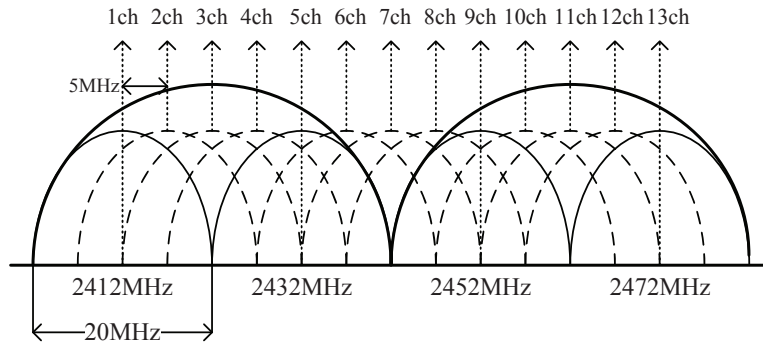


Figure 2.10: IEEE 802.11n channel bonding concept.

- *Frame Aggregation:*

In the frame aggregation, multiple data frames can be transmitted in one packet with a single pre-amble and header information to reduce the protocol overheads, and thereby increases the user level data rate [59]. In the IEEE 802.11n protocol, the *MAC protocol data unit (A-MPDU)* aggregation and the *MAC service data unit (A-MSDU)* aggregation are available.

- *Modulation and Coding Scheme:*

Various modulation, error-correcting codes are used in IEEE 802.11n, represented by a Modulation and Coding Scheme (MCS) index value, or *mode*. IEEE 802.11n defines 31 different modes and provides the greater immunity against selective fading by using the Orthogonal Frequency Division Multiplexing (OFDM). This standard increases the number of OFDM sub-carriers of 56 (52 usable) in *High Throughput (HT)* with 20MHz channel width and 114 (108 usable) in HT with 40MHz . Each of these sub-carriers is modulated with BPSK, QPSK, 16-QAM or 64-QAM, and Forward Error Correction (FEC) coding rate of $1/2$, $2/3$, $3/4$ or $5/6$ [59].

- *Short Guard Interval:*

Guard Interval (GI) between two successful OFDM symbols is reduced from 800ns to short GI of 400ns to further improve the throughput.

Table 2.4 shows the relationships between the maximum throughput (*Mbps*), the number of spatial streams with MIMO links, the channel width, and GI [5].

Table 2.4: Effects of channel width, MIMO links and guard interval on IEEE 802.11n’s throughput.

# of Spatial Streams	Throughput (<i>Mbps</i>)			
	20 MHz Channel		40 MHz Channel	
	800 ns GI	400 ns GI	800 ns GI	400 ns GI
1	65	72.2	135	150
2	130	144.4	270	300
3	195	216.7	405	450
4	260	188.8	540	600

2.3.1 Link Speed Change Feature of IEEE 802.11n MIMO Links

The throughput performance of the IEEE 802.11n link is affected by many factors including the type of AP or PC, the transmission power of AP, MCS, the link distance between AP and host, and the design of network adapters. In our preliminary experiments [21], we measured the link speed when both end nodes adopted the IEEE 802.11n MIMO protocol and the distance between them is increased from 1m to 170m with the 5m interval in a free space. As shown in Figure 2.11, the link speed gradually decreases as the distance increases. Because, the RSS drops with distance and lower modulation and coding schemes (MCSs) are adopted.

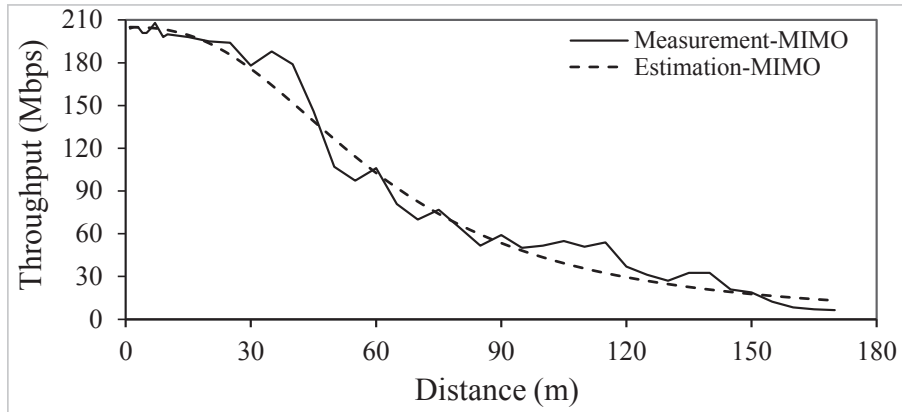


Figure 2.11: Link speed change for IEEE 802.11n 2 × 2 MIMO link.

Then, we approximated this link speed change features of the IEEE 802.11n MIMO link, S_h by the *sigmoid function* as follows:

$$S_h = \frac{205}{1 + e^{-\left(\frac{P_d+120}{4.8}\right)-49}} \quad (2.2)$$

where P_d represents the receiving signal strength (RSS) at the receiver host which is estimated using the *log-distance path loss model*, and S_h does the estimated link speed (throughput) at the host from the AP. The estimated result using this equation is also plotted by the dashed line in Figure 2.11.

2.4 IEEE 802.11ac Protocol

IEEE 802.11ac is an improvement to the IEEE 802.11 2007 wireless network standard that operates only 5 GHz frequency band, supports 160MHz channel widths, multiuser MIMO (MU-MIMO), the increased number of spatial streams, and the higher order of modulations over the previous standard [48, 54, 55]. Table 2.5 shows a brief summary of the 802.11ac standard.

Table 2.5: Specification of IEEE 802.11ac.

Specification	IEEE 802.11ac	
Frequency Band	5 GHz	
Available Channel	19 ch	
Simultaneous Uninterrupted Channel	9 ch	
Max. Throughput	6.93Mbps	
Max. # of Spatial Streams	8	
Max. Modulation Types	256 QAM	
Max. Coding Rate	5/6	
Max. Channel Width	160 MHz	
Guard Interval	800 ns	400 ns
Release Date	December 2012	

IEEE 802.11ac uses the same WiFi channels with IEEE 802.11n at 5 GHz, as shown in Figure 2.8. In this frequency band, there are nine simultaneous uninterrupted channels using the 40MHz bandwidth free from the channel overlapping and interference between each other. For the 80MHz bandwidth, which doubles the channel width, there are four channels. For the 160MHz bandwidth, there are two. The IEEE 802.11ac WiFi channels are the same with the IEEE 802.11n at 5 GHz, as shown in Figure 2.8.

The channel bonding can increase the data transmission capacity by bonding two or more adjacent channels into one channel. IEEE 802.11ac allows to bond maximally eight 20MHz channels into one 160MHz channel. Due to channel bonding, IEEE 802.11ac can use up to 468 sub-carriers at the 160MHz channel. The previous IEEE 802.11n does 108 sub-carriers at the 40MHz channel[60]. This sub-carrier increase can also enhance the data capacity by more than twice.

It is noted that, within a crowded environment, if multiple APs are in use, the non-overlapping channels will drop down to 9, 4, and 2 channels when using channel bonding for the bandwidth of 40MHz, 80MHz, and 160MHz respectively. In order to avoid interferences between APs, the lower channel bandwidth will provide the fairer performance for users. Table 2.6 shows the usage of the different channel bandwidth and spatial stream towards the throughput of IEEE 802.11ac [61].

In IEEE 802.11ac, eight spatial streams can be used to transmit up to 866.7 Mbps/stream and reach the maximum data rate (throughput) of 6,933 Mbps through the MIMO technology. MIMO can transmit multiple data in parallel by adopting multiple antennas. For example, when the source

Table 2.6: Effects of channel bandwidth, spatial streams, and GI on IEEE 802.11ac's throughput.

# of Spatial Streams	Throughput (<i>Mbps</i>)			
	20 MHz Channel	40 MHz Channel	80 MHz Channel	160 MHz Channel
1	86.7	200	433.3	866.7
2	173.3	400	866.7	1733.4
3	288.9	600	1300	2600
4	346.7	800	1733.2	3466.8
8	693.4	1600	3466	6933

node and the destination node have two antennas respectively, the transmission speed becomes doubled using two data streams. IEEE 802.11ac allows the maximum of eight antennas.

Besides, IEEE 802.11ac comes with MU-MIMO, which allows an AP to transmit data to multiple hosts in a parallel way without interferences between them by adopting the beamforming technology that generates directional radio signals. This is far faster than the serial communication in IEEE 802.11n. MU-MIMO can realize 1-to-n data transmissions using the same band.

Apart from MU-MIMO, IEEE 802.11ac also introduces the beamforming technology. In beamforming, a sender detects the location of the receiver and transmits data through intensifying the signal in this direction. The focus of the radio frequency energy towards the receiver will provide the higher signal strength to increase the speed. This is better than the traditional way of broadcasting wireless signals equally in Omni directions [49]. Figure 2.12 shows the difference between the usage of beamforming technology and normal WiFi.

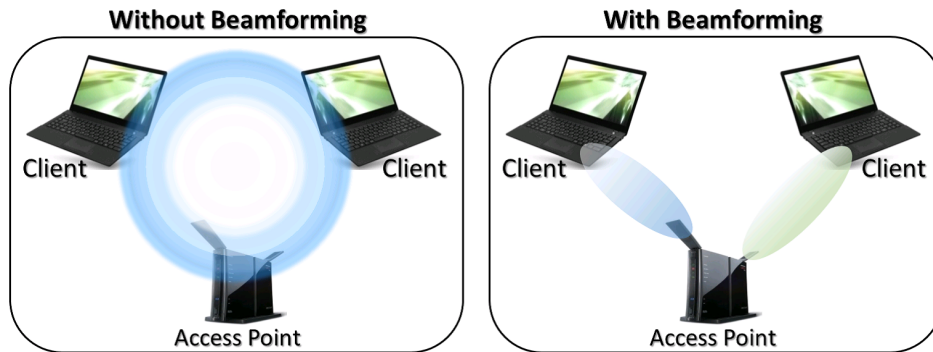


Figure 2.12: Beamforming technology.

IEEE 802.11ac inherits A-MSDU and A-MPDU from IEEE 802.11n, and allows the maximum of 1 Mbyte for one frame, whereas IEEE 802.11n does 64 Kbyte.

In order to gain the higher transmission rate, the *Guard Interval (GI)* that represents the period between two consecutive packet transmissions has been reduced. It is necessary to avoid interferences between them that can be caused by the delay of the first packet arrives at the destination node. IEEE 802.11ac adopts 400 ns as the guard interval time, whereas IEEE 802.11a/g does 800 ns.

In the physical layer, IEEE 802.11ac use the 256 QAM scheme under MCS. In 256 QAM, eight bits of input alters the phase and amplitude of the carrier to generate 256 modulation states. Figure 2.13 shows the comparison between 64 QAM constellation (IEEE 802.11n) to the 256

QAM constellation.

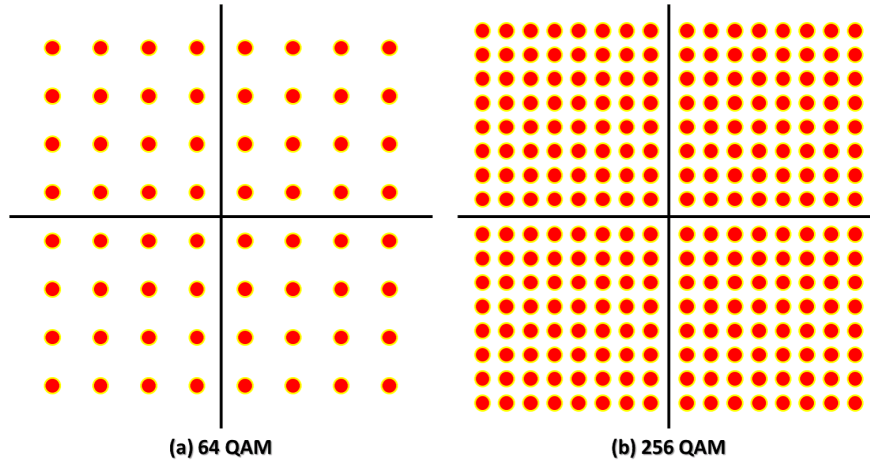


Figure 2.13: Comparison of modulation.

2.5 Commercial and Software APs

In WLAN, the *access point (AP)* is the networking device that acts as the central trans-receiver or base station. It allows one WiFi devices to connect with each other within the network and serves as the interconnection point between WLAN and the wired network. Each AP can support the connection of multiple wireless devices.

A lot of commercial APs from different vendors are now available for WLAN. In Japan, APs from Buffalo, I-O data, and NEC are popular [62–64]. They can operate in both IEEE 802.11n and 11ac protocols. According to our measurements, the AP from NEC usually has the largest throughput of around 210 *Mbps* for a PC with 2×2 MIMO in the outdoor environment. However, this peak throughput varies significantly depending on the propagation environment including the obstacles, the channel interference, the number of antennas, the transmission power of AP, the Wi-Fi adapter, and the placement height and orientation angle of AP.

Recently, the *software enabled AP (SoftAP)* is popular in IEEE 802.11n WLAN. A laptop/PC user can be used as an AP by installing the software of AP functions using hostapd software [13]. Along with this trend, *Raspberry Pi* device can be a good choice for the device to run as a software AP. It provides the cost-effective, energy saving, and card-sized portable embedded system. The price of one Raspberry Pi (35-40 USD) is only one-tenth of a laptop PC and it consumes the much less power (5V) [65, 66]. WiFi devices can be connected to this SoftAP in the same way to a commercial AP.

Raspberry Pi is basically adopted Raspbian, a Debian based Linux distribution as the OS and has the built-in wireless network interface card (NIC) which has only one antenna. This built-in NIC in Raspberry Pi supports only 20MHz channel for data transmission since its internal circuitry does not permit 40MHz channel bonding functionality. According to our experiment using Raspberry Pi with built-in NIC, the peak throughput becomes about 40*Mbps*. To improve the performance, an external USB MIMO or SISO adapter can be used in Raspberry Pi which can realize hardware channel bonding.

2.6 Summary

In this chapter, we presented various technology features of IEEE 802.11n/ac protocols, commercial and software WLAN devices, which are adopted in this thesis for our experiments, throughput estimation models, as well as simulations. In the next chapter, we will review our previous related studies.

Chapter 3

Review of Previous Studies

In this chapter, we briefly overview our previous studies related to this thesis. First, we review the study of the throughput estimation model for IEEE 802.11n link in WLAN. Next, we review that of the elastic WLAN system. Finally, we review that of the active AP configuration algorithm for the elastic WLAN system.

3.1 Throughput Estimation Model for IEEE 802.11n Link

In this section, we review the throughput estimation model for IEEE 802.11n link in WLAN.

3.1.1 Overview

This model estimates the link speed or data throughput of an IEEE 802.11 link in WLAN. It has two main steps to estimate the throughput between a source and a destination node. In the first step, it estimates the *receiving signal strength (RSS)* at the host by using the *log distance path loss model*. In the second step, it converts the estimated *RSS* into the corresponding throughput by the *sigmoid function* [14]. Both functions have several configuration parameters that can affect the estimation accuracy, which depends on link specifications and network field environments.

3.1.2 Receiving Signal Strength Estimation

The signal strength is estimated by the log-distance path loss model and it considers the multi-path effects by considering both the direct signal along the line of sight (*LoS*) and indirect signal through non line of sight (*NLoS*) path in indoor environments.

3.1.2.1 Log Distance Path Loss Model

The *RSS*, P_d (*dBm*), at the host is estimated using the *log distance path loss model* by considering the distance and the obstacles loss between end nodes[67]:

$$P_d = P_1 - 10\alpha \log_{10} d - \sum_k n_k W_k \quad (3.1)$$

where P_1 represents the signal strength at 1m from the AP (source), α is the path loss exponent, d (m) does the link distance from the AP, n_k does the number of the type- k walls along the path between the AP and the host, and W_k does the signal attenuation factor (*dBm*) for the type- k wall

in the environment. The estimation accuracy of *RSS* relies on the parameter values, which depend on the propagation environment [67].

For indoor environments, five wall types have been considered. Namely, W_1 represents the *corridor wall* made of concrete that has the sufficient strength to support the structure. W_2 does the *partition wall* that separates the successive rooms. The *intervening wall* W_3 signifies the concrete wall that has the sufficient strength but does not separate closed rooms. W_4 represents the *steel wall* of the elevator, and W_5 does the *door wall* composed of metals and glasses.

3.1.2.2 Multipath Effect

Due to the *multipath effect* in indoor environments, the receiver may receive the *indirect signal* through *NLoS* path that arrives after reflected/diffracted at some points on walls or obstacles, in addition of the *direct signal* along the *LOS* path. When the direct signal passes through multiple walls, the *RSS* becomes weaker than that of the indirect signal if it passes through much fewer walls.

In the throughput estimation model, we consider this multi-path effect by selecting a *diffraction point* for each AP/host pair such that it is located on the wall in the same room as the host and *RSS* of the AP is largest. The indirect signal reaches the host through this diffracting point after the signal is attenuated there. The *RSS* through indirect path, P_{ind} is calculated by:

$$P_{dif} = P_1 - 10\alpha \log_{10} r - \sum_k n_k W_k \quad (3.2)$$

$$P_{ind} = P_{dif} - 10\alpha \log_{10} t - W_{dif} \quad (3.3)$$

where P_{dif} represents the *RSS* at the diffraction point, r (m) is the distance between the AP and the diffraction point, t (m) does the distance between the diffraction point and the host, and W_{dif} (dBm) does the attenuation factor at the diffraction point. For the estimated *RSS* at the receiver, the larger one between the direct or indirect signals is selected.

3.1.3 Throughput Conversion by Sigmoid Function

From the *RSS*, the throughput S ($Mbps$) of the link is derived using following the *sigmoid function*:

$$S = \frac{a}{1 + e^{-\left(\frac{(P_d+120)-b}{c}\right)}} \quad (3.4)$$

where a , b , and c are the constant parameters of the sigmoid function that should be optimized by parameter optimization tool [25]. The assumption of this sigmoid function for the throughput estimation is based on our real-world measurement results which clearly reflects the relationship between the *RSSs* and the estimated throughput.

3.1.4 Parameter Optimization Tool

The parameter optimization tool is used to explore the optimal parameter values for the throughput estimation model based on a local search method that jointly uses the tabu table and the hill climbing search to avoid a local minimum convergence [25]. This tool searches the parameter values in a way that minimize the throughput estimation error. For the accurate throughput estimation, it plays a vital role, which is essential for the efficient WLAN design.

3.1.5 Procedure for Throughput Estimation

According to [14], the procedure for the throughput estimation model is as follows:

- (i) First, the parameter values of the throughput estimation model are optimized by applying the parameter optimization tool [25].
- (ii) Then, the Euclidean distance, $d(m)$ for each link between the AP/host pair is calculated and identify the link that crosses with each type of wall in the network field.
- (iii) For the direct signal, the RSS at the host is estimated using *Eq. (3.1)*.
- (iv) And for the indirect signal, the RSS at the host is calculated using *Eq. (3.2)* and *Eq. (3.3)*.
- (v) Then, we select the larger RSS between the direct and indirect signal for the sigmoid function.
- (vi) Finally, the throughput, S (*Mbps*) is estimated from the RSS using *Eq. (3.4)*.

3.2 Elastic WLAN System

In this section, we briefly review the elastic WLAN system, which can dynamically optimize the network configuration by activating/deactivating APs, according to traffic demands and network situations [11, 12].

3.2.1 Overview

The elastic WLAN system dynamically controls the number of active APs in the network by activating or deactivating the installed APs according to traffic demands and network conditions. Figure 3.1 illustrates an example topology of the elastic WLAN system.

3.2.2 Implementation

The implementation of the elastic WLAN system adopts the *management server* to manage and control the APs and the hosts. This server not only has the administrative access to all the devices in the network, but controls the whole system through the following three steps:

1. The server explores all the devices in the network and collects the requisite information for the active AP configuration algorithm.
2. The server executes the active AP configuration algorithm using the inputs derived in the previous step. The output of the algorithm contains the list of the active APs, the host associations, and the assigned channels.
3. The server applies this output to the network by activating or deactivating the specified APs, changing the specified host associations, and assigning the channels.

3.3 Active AP Configuration Algorithm

In this section, we briefly review the AP configuration algorithm for the elastic WLAN system that optimizes the number of active APs and the host associations.

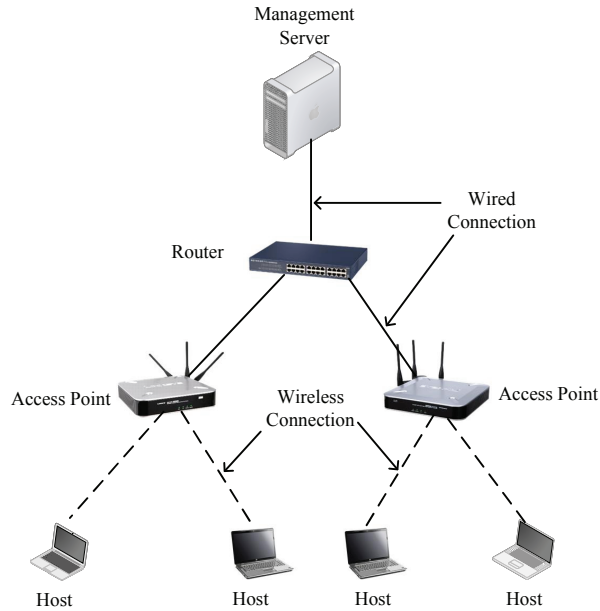


Figure 3.1: Elastic WLAN system topology.

3.3.1 Problem Formulation

The active AP configuration problem for this algorithm was formulated as follows:

1. Inputs:

- Number of hosts: H
- Number of APs: $N = N^D + N^V + N^M$ where N^D , N^V , and N^M represent the number of DAPs, VAPs, and MAPs respectively.
- Link speed between AP_i and $host_j$ for $i = 1$ to N , $j = 1$ to H : s_{ij} , where the link speed can be estimated by the model in [14].
- Minimum link speed for association: S
- Number of non-interfered channels: C

2. Outputs:

- Set of active APs
- Set of hosts associated with each active AP
- Channel assigned to each active AP

3. Objectives:

- To minimize E_1 .
- Holding the first objective, to maximize E_2 .
- Holding the two objectives, to minimize E_3 for channel assignments.

Let, E_1 represents the number of active APs (DAPs, VAPs, and MAPs) in the network:

$$E_1 = E_1^D + E_1^V + E_1^M \quad (3.5)$$

where E_1^D represents the number of active DAPs, E_1^V does the number of active VAPs, and E_1^M does the number of active MAPs respectively.

The transmission delay of the j th AP can be defined by:

$$T_j = \sum_{k \in \mathcal{P}_j} \frac{D_k}{s_{jk}} \quad (3.6)$$

where D_k represents the traffic of the k th host, s_{jk} does the link speed between the j th AP to the k th host, and \mathcal{P}_j does the set of the hosts associated with the j th AP.

Then, the average throughput TH_{ij} of the i th host associated with the j th AP can be estimated by:

$$TH_{ij} = \frac{D_i}{T_j} = \frac{D_i}{\sum_{k \in \mathcal{P}_j} \frac{D_k}{s_{jk}}} \quad (3.7)$$

Since the real traffic of each host is unpredictable, we assume the identical traffic for every host, which can be represented by the unit traffic for the sake of simplicity. Then, the average host throughput for AP_j is given by:

$$TH_j = \frac{1}{\sum_{k \in \mathcal{P}_j} \frac{1}{s_{jk}}} \quad (3.8)$$

If $TH_j \geq G$, the minimum host throughput constraint is satisfied, where G represents the threshold for this constraint. Then, the second objective function E_2 is defined to maximize the *minimum average host throughput* for the bottleneck, AP which is given by:

$$E_2 = \min_j [TH_j] \quad (3.9)$$

E_3 signifies the total interfered communication time:

$$E_3 = \sum_{i=1}^N [IT_i] = \sum_{i=1}^N \left[\sum_{\substack{k \in I_i \\ c_k = c_i}} T_k \right] \quad (3.10)$$

where IT_i represents the *interfered communication time* for AP_i , T_i does the *total communication time* for AP_i , I_i does the *set of the interfered APs* with AP_i , and c_i does the *assigned channel* to AP_i . They are given by follows:

- T_k is given by the sum of the time that is required to transmit one bit between AP_k and its each associated host.
- I_i represents the set of the indices of the APs that are interfered with AP_i if they are assigned the same channel.

- c_k signifies the channel assigned to AP_k by the active AP configuration algorithm.
- IT_i is given by the sum of the total communication time for the APs that are interfered with AP_i .

4. Constraints:

- Minimum host throughput constraint: each host in the network must enjoy the given threshold G on average when all the hosts are communicating simultaneously.
- Bandwidth limit constraint: the bandwidth of the wired network to the Internet must be less than or equal to the total available bandwidth of the network B^a .
- Channel assignment constraint: each AP must be assigned one channel between 1 and C .

3.3.2 Algorithm Procedure

The active AP configuration algorithm consists of three phases: *active AP and associated host selection phase*, *channel assignment phase*, and *channel load averaging phase*.

3.3.2.1 Active AP and Associated Host Selection Phase

In this phase, the set of the active APs and their associated hosts are selected. This phase comprises following eight steps:

1. Preprocessing

The link speed for each possible pair of an AP and a host is estimated with the measurement or the throughput estimation model [14]. Then, this step initializes the variables for the following steps:

- For each AP, make a list of hosts that can be associated with this AP, where the throughput of the link between a host and an AP is S or larger, it can be associated. This list is called the *associable host list for APs*.
- Initialize each AP as the *non-active AP*. Initially, only the DAPs are selected as *candidate APs*.

2. Initial Solution Generation

An initial solution to the cost function E_1 is derived using a greedy algorithm, which repeats the following procedures:

- Select the AP that can be associated with the maximum number of non-associated hosts.
- Activate this AP and increment E_1 by one.
- Update the number of non-associated hosts in the host list for APs.

3. Host Association Improvement

The cost function E_2 is calculated for the greedy solution using Eq. (5.1). Then, this solution is improved by repeating the following procedure:

- (a) Find the AP that gives the lowest host throughput in Eq. (5.1).
- (b) Select one host randomly from the associated hosts with this AP, and associate it with another active AP that is selected randomly. Then, calculate E_2 .
- (c) Keep the new association only if this new E_2 is higher than the previous E_2 . Otherwise, return to the previous association.

4. AP Selection Optimization

The cost functions E_1 and E_2 are further jointly improved in this step under the constraints mentioned before by the *local search* [68]. This local search repeats the following three procedures:

- (a) If the current solution satisfies the *minimum host throughput constraint*, it seeks to reduce the number of active APs E_1 by deactivating an active AP. In the implementation, it repeats to 1) randomly select an active AP and deactivate it, 2) apply *Host Association Improvement*, and 3) check the feasibility of this deactivation.
- (b) Otherwise, it seeks to improve the *minimum average host throughput* E_2 with the same number of active APs by changing the active AP. In the implementation, it repeats to 1) randomly select a non-active AP and activate it, 2) apply *Host Association Improvement*, and 3) check the possibility of deactivating another active AP.
- (c) If (b). is not achieved, it seeks to satisfy the *minimum host throughput constraint* by increasing the number of active APs while improving the *minimum average host throughput*. In the implementation, it 1) randomly selects a non-active AP and 2) applies *Host Association Improvement*.

5. Link Speed Normalization

The fairness criterion will be applied when the total expected bandwidth exceeds B^a . Generally, the link speed is normalized as:

- (a) Calculate the expected total bandwidth B^e by the summation of the throughputs of all the APs.
- (b) If $B^e > B^a$, adjust each AP-host link speed as:

$$\hat{s}_{ij} = s_{ij} \times \frac{B^a}{B^e} \quad (3.11)$$

where \hat{s}_{ij} is the normalized link speed.

6. Termination Check

The algorithm is terminated when either of the following conditions is satisfied:

- (a) The *minimum host throughput constraint* is satisfied.
- (b) All the APs in the network have been activated.

7. Additional VAP Activation

If all the DAPs become active but the *minimum host throughput constraint* is still not satisfied, VAPs are newly selected as candidate APs. A VAP is slower than a DAP, but faster than a MAP. The locations of hosts are considered as the locations of the candidate VAPs, because user hosts may be used for VAPs. Then, it returns to *AP Selection Optimization* step.

8. Additional MAP Activation

If all the DAPs and VAPs become active but the *minimum host throughput constraint* is still not satisfied, MAPs are newly selected as candidate APs. A MAP is the slowest among the three AP types. The locations of hosts are considered as the locations of the candidate MAPs, because users may have MAPs. Then, it returns to *AP Selection Optimization* step.

3.3.2.2 Channel Assignment Phase

In this phase, the assigned channels to the active APs are selected and it has the following four steps:

1. Preprocessing

The interference and delay conditions of the network are represented by a graph.

- (a) Construct the *interference graph*, $G = (V, E)$, from the APs and the hosts, where the vertex V represents the set of APs and the edge E presents the existence of the interference between two APs. $e(i, j) \in E$ if AP_i is interfered with AP_j in the network.
- (b) Calculate the *communication time* for each AP. The communication time T_i for AP_i is defined as the total time when the AP transmits 1-bit to all the associated hosts. It is given by:

$$T_i = \sum_j \frac{1}{sp_{ij}} \quad (3.12)$$

where sp_{ij} represents the link speed between AP_i and $host_j$.

- (c) Calculate the *neighbor interfered communication time* for each AP. The neighbor interfered communication time NT_i for AP_i is given by:

$$NT_i = \sum_{e(i,k)=1} T_k \quad (3.13)$$

2. Interfered AP Set Generation

The set of APs that are interfering with each other is found for each AP.

- (a) Sort the APs in descending order of NT_i , where the tie-break is resolved by T_i .
- (b) Find the interfered AP set for each AP by repeating the following steps:
 - i. Initialize the interfered AP set by $I_i = \{i\}$ for AP_i .
 - ii. Expand I_i by examining the APs in sorted order in a) whether the AP is interfered with each AP in I_i . If so, include this AP, AP_j , into I_i , i.e. $I_i = I_i \cup \{j\}$.
- (c) Calculate the total interfered communication time AT_i for AP_i , which is given by:

$$AT_i = \sum_{k \in I_i} T_k \quad (3.14)$$

3. Initial Solution Construction

Then, an initial solution is derive with a greedy algorithm.

- (a) Sort the APs in descending order of the total interfered communication time AT_i , where the tie-break is resolved by NT_i .

- (b) Assign a channel c to AP_i such that the interfered communication time IT_i is minimized if it is assigned. IT_i is given by:

$$IT_i = \sum_{\substack{k \in I_i \\ c_k = c_i}} T_k \quad (3.15)$$

where c_k represents the assigned channel to AP_k .

- (c) Repeat 2) until each active AP is assigned to one channel.
(d) Calculate the cost function E_3 using Eq. (3.10) and save this initial solution as the best solution E_3^{best} .

4. Solution Improvement by Simulated Annealing

Finally, the initial solution is improved by repeating the following *simulated annealing (SA)* procedure with the constant *SA temperature* T^{SA} for the *SA repeating times* R^{SA} , where T^{SA} and R^{SA} are given algorithm parameters:

- (a) Randomly select one AP and one new channel for the channel change trial.
(b) Calculate the interfered communication time IT_i after assigning this new channel by:
(c) Calculate E_3^{new} using Eq. (3.10) for the new channel assignment, and $\Delta E_3 = E_3^{new} - E_3$.
(d) If $\Delta E_3 \leq 0$, accept the new channel assignment, and address this new solution as the best one.
(e) Otherwise, generate a 0-1 random number, *rand*, and if $rand \leq \frac{-\Delta E_3}{T^{SA}}$, then accept the new channel assignment.

3.3.2.3 Channel Load Averaging Phase

After the channel assignment using the limited number of channels, the total loads may be imbalanced depending on different channels that are assigned to the APs. In this phase, the channel load is averaged by changing associated APs for hosts. It has four steps as follows:

1. Preprocessing

The *AP flag* for each AP is initialized with *OFF* to avoid processing the same AP.

2. AP Selection

One AP is selected to move its associated host to a different AP that is assigned a different channel.

- (a) Terminate the procedure if each AP has *ON* AP flag.
(b) Initialize the host flag by *OFF* for each host.
(c) Select one AP, say AP_i , that satisfies the two conditions:
i. The AP flag is *OFF*.
ii. The interfered communication time IT_i is largest among the *OFF* APs.
(d) Set the AP flag *ON*.

3. Host Selection

Then, one host associated with AP_i is selected for the associated AP movement.

- (a) Select one host, say H_j , that satisfies the four conditions:
 - i. The host flag is *OFF*.
 - ii. The host is associated with AP_i .
 - iii. The host can be associated with another AP assigned a different channel from AP_i , or is located out of the interference range of AP_i .
 - iv. The link speed with AP_i is the smallest among the hosts satisfying (a)–(c).
- (b) If one host is selected, set the host flag *ON*.
- (c) Otherwise, return to *AP Selection* for the new AP selection.

4. Association Change Application

Finally, the new associated AP is selected for H_j .

- (a) Select the AP that has the largest link speed among the APs that are assigned to a different channel from AP_i and can be associated with H_j .
- (b) Calculate the new cost function E_3^{new} with Eq. (3.10) if H_j is associated with this AP.
- (c) If E_3^{new} is equal to or smaller than the previous E_3 , accept the new association, and return to *Host Selection*.
- (d) Otherwise, select another AP that has the next largest link speed, and return to 3).
- (e) If no such AP exists, return to *Host Selection* for the new host selection.

3.4 Summary

In this chapter, we reviewed the previous works of the throughput estimation model in WLAN, the elastic WLAN system, and the active AP configuration algorithm. In the next chapter, we will present the throughput measurement results for IEEE 802.11n MIMO/SISO links under various conditions in indoor and outdoor environments, and extend the throughput estimation model by considering the concurrent communications of multiple hosts with a single AP.

Chapter 4

Throughput Measurements and Estimation Models under Various Conditions

In this chapter, we present *throughput measurement results* under a variety of indoor and outdoor environments, and two modifications to the *throughput estimation model* for concurrent communications of multiple hosts with a single AP, which will be used in the *MIMO host location optimization approach* for the active AP configuration algorithm.

4.1 Introduction

The demands for the high-speed Internet access has always been issues in WLAN systems. The user in WLAN may perform various high-load jobs such as downloading bulk files and watching live videos, simultaneously [69]. To meet these demands, the analysis and the estimation of the throughput performance of a WLAN system are very important for improving and/or developing protocols or algorithms for a WLAN system.

To optimize the performance of a WLAN system, we study the *MIMO host location optimization algorithm* as an extension of the *active AP configuration algorithm* [27]. For this MIMO host location optimization algorithm, whose details will be presented in Chapter 5, the accurate throughput estimation of a WLAN MIMO/SISO link is crucial. During the optimization process, the throughput must be estimated repeatedly every time a user host is located at a different location in the network field. By repeating this throughput estimation, the design of a WLAN system can be improved with low costs before its actual deployment.

Especially, in the indoor environment, the accurate estimation of the throughput becomes much harder from that in the outdoor environment, due to the signal attenuations by different types of walls, floors, and other obstacles [15, 16], where multipath effects should also be considered. The accurate throughput estimation needs to properly handle the floor plan, the materials and the thickness of the walls, and the multi-path effect. A network designer needs to carefully select these parameter values for the accurate throughput estimation for a WLAN MIMO/SISO link in a real environment.

Furthermore, the *concurrent communication* between multiple hosts and a single AP, which often appears in a practical network, offers different the throughput features from the *single communication* between a single host and an AP. In this case, the packet collisions due to the interferences increase with the number of concurrent communicating hosts per AP [17]. Besides, the hosts with the stronger RSS may occupy the frequency channel for a long time, which causes the

unfairness among the hosts. This effect of the concurrent communication must be also considered in the throughput estimation.

4.2 Experiment Setups

In this section, we describe the experimental setup for throughput measurements including the network fields, adopted devices, and software tools.

4.2.1 Devices and Software Tools

The measurements were conducted using one PC for the server and six laptop PCs for the user hosts. Among six PCs, only one can use 2×2 MIMO for the *IEEE 802.11n network interface card (NICs)*, while others can use 1×1 SISO. The AP supports *IEEE 802.11n* at $2.4GHz$. The server PC is connected to the AP via the $1Gbps$ wired (Ethernet) link, and the host PC is associated with the AP via a wireless (Wi-Fi) connection. In the measurements, we adopt following two types of APs:

- *Commercial dedicated AP: NEC WG2600HP* [62]: This AP accepts up to 3×3 MIMO with four internal antennas. It supports the maximum transmission rate (standard value) of $300Mbps$ with the two-streams or $150Mbps$ with one stream using the $40MHz$ channel and the $400ns$ GI mode. Therefore, the maximum transmission rate for the link between this AP and a host is $300Mbps$ or $150Mbps$.
- *Software AP : Broadcom BCM2837 Raspberry Pi3* [70]: This AP is configured as a *IEEE 802.11b/g/n* software AP [23] using *hostapd*. It uses *Raspbian OS* for the operating system and the in-built (NIC) with 1×1 internal antenna supporting IEEE 802.11n. In addition, 2×2 MIMO USB adapters are adopted for *Raspberry Pi3*.

iperf 2.05 [71] software is used to measure the throughput by generating $50s$ *transmission control protocol (TCP)* traffics with the $477KB$ TCP window size and the $8KB$ buffer size. Besides, *Homedale* [72] network monitoring tool is used at the host PC to measure the *RSS* from the AP.

Before measurements, first, all the unessential startup programs are disabled in the operating system and the configuration of the network adapter is optimized by running the *SG TCP optimizer* [73] tool. Then, the channel condition at $2.4GHz$ in our network field is checked by using *Homedale* network monitoring tool. Then, the channel 11 (ch 9 + ch 13) is selected to form the $40MHz$ channel bonding for our measurements, which is the lowest interfered channel observed in the network field. Figure 4.1 shows the measurement setup. Table 4.1 shows the specifications of devices and software tools used for our measurements.

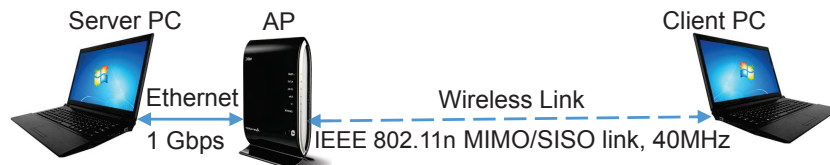


Figure 4.1: Simple network configuration for measurement.

Table 4.1: Devices and software in measurements.

server PC	model	Lesance W255HU
	CPU	Intel(R) Core i5 2450M (2.50 GHz)
	network adapter	JMicron JMC250 Gigabit Ethernet
	OS	Windows 7
MIMO host PC	model	Lenovo ThinkPad E560 20EVCTo1
	CPU	Intel(R) Core i5-3317U (2.3GHz)
	# of antennas	2
	wireless adapter	Intel(R) Dual Band Wireless-AC 8260
SISO host PC	model	Ultrabook Lesance NB S344/L
	CPU	Intel(R) Core i5-3317U (1.7GHz)
	# of antennas	1
	wireless adapter	Qualcomm Atheros AR9285
Commercial AP	model	NEC WG2600HP
	Operating mode	IEEE802.11n (MIMO)
	# of antennas	4
	Channel width	40MHz
Software AP	model	Broadcom BCM2837 Raspberry Pi (1.2GHz)
	Operating mode	IEEE802.11n (SISO/MIMO)
	# of antennas	1 (built-in NIC adapter), 2 (USB MIMO adapter)
	Channel width	20MHz/40MHz
Software and Protocol	iperf 2.05	Throughput measurement [71]
	Homedale	RSS measurement [72]
	SG TCP optimizer	To tune and optimize network adapters [73]

It is noted that all the experiments are conducted on weekends to reduce the interferences from other APs in the same environment. The experiment under each condition was repeated five times to take the average of the measured throughputs.

4.2.2 Network Fields

The three network fields in Figure 4.2 are adopted in our experiments. The *triangle* represents the AP location, and the *rectangle* does the host location. The *field#1* represents the outdoor environment, which is actually the river bed of Asahi River in Okayama city, where almost no interfering signal was observed. The *field#2* and the *field#3* are situated in the indoor environments. The *field#2* represents the 3rd floor of Engineering Building#2 and the *field#3* does the 2nd floor of Graduate School Building in Okayama University, Japan. Each room in these fields is surrounded by walls with different thickness and materials. In the indoor environments, two different scenarios are considered, namely the *line-of-sight (LoS) scenario* at the corridor, and the *non-line-of-sight (NLoS) scenario* at several rooms. In these network fields, various experiments are conducted by considering 1) a single host communication with the AP at a time, and 2) concurrent host communications by multiple hosts with an AP.

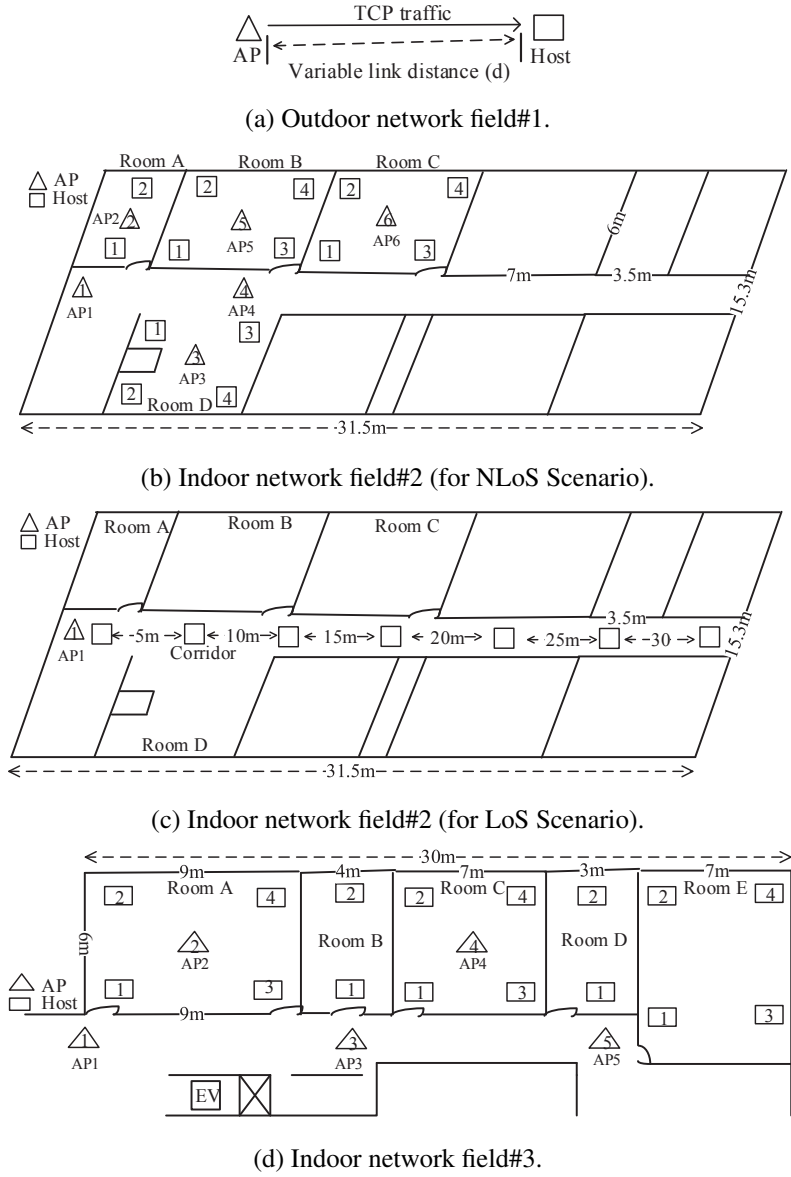


Figure 4.2: Three network fields.

4.3 Results for Commercial AP

In this section, we show the measurement results of the RSS and the throughput, and also the estimated throughput by the throughput estimation model [14], when a single IEEE 802.11n MIMO/SISO PC for the user host is communicating with the commercial dedicated AP in the outdoor and indoor environments.

4.3.1 Results in Outdoor Environment

First, we show the evaluation results in the *field#1* for the outdoor environment.

1. *Measurement Results in Outdoor:* Figure 4.4 shows the RSS and throughput measurement results for the 2×2 MIMO link and the 1×1 SISO link in the *field#1*, when the distance between the AP and the host increases from $0m$ to $170m$ with the $5m$ interval in the LoS



Figure 4.3: Position of host in outdoor network field (field#1).

scenario. Figure 4.3 (source from Google, maps.google.com) shows the position of the host from 0m to until 170m in the river bed of Ashai river, Okayama city.

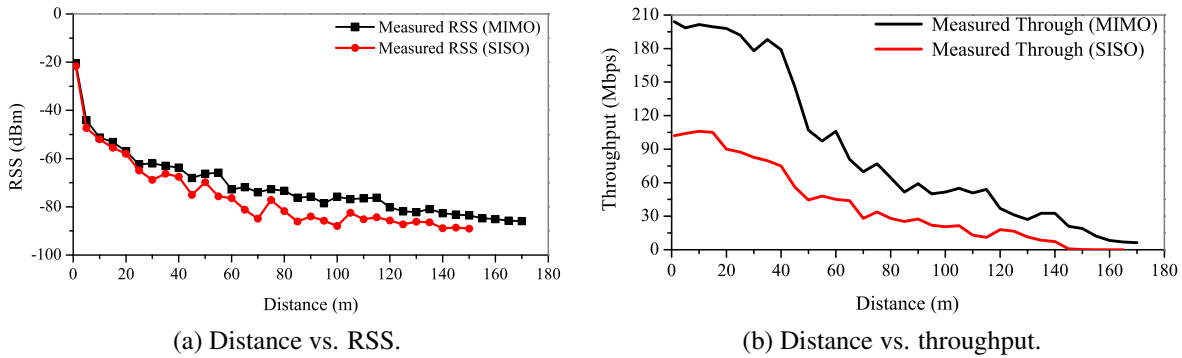


Figure 4.4: Measurement results for 2×2 MIMO and SISO links.

From Figure 4.4, it is observed that the throughput gradually decreases as the distance increases, since the *RSS* declines and the slower *modulation and coding scheme (MCS)* is adopted. The lower *RSS* implies the poor *signal-to-noise ratio (SNR)* at the receiver, and causes the higher errors. The throughput measurement results are stepwise due to the changes of adopted *MCS* with the distance.

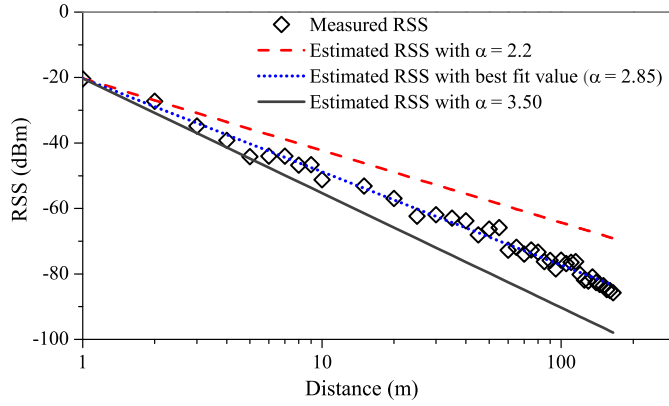
It is also observed that the usable range of 2×2 MIMO link is higher than the SISO link, and the maximum (peak) throughput becomes around doubled compared to that of the SISO link with the single antenna. The multiple antennas in the MIMO link provides the better link quality and the higher reliability for the link between the transmitter and the receiver.

2. *Estimation Model Parameters*: Then, the values of the model parameters are tuned by the *parameter optimization tool* using the measurement data. Table 4.2 shows the parameter values for the 2×2 MIMO link and the 1×1 SISO link in the outdoor environment found by the tool. Figure 4.5a shows the change of *RSS* with respect to the distance for the 2×2 MIMO link in the *field#1*. Figure 4.5b does the relationship between the measured *RSS* and the throughput. From Figure 4.5a, $P_1 = -20.3$ and $\alpha = 2.85$ are derived. From Figure 4.5b, $a = 205$, $b = 49.0$, and $c = 4.8$ are derived for the MIMO link.

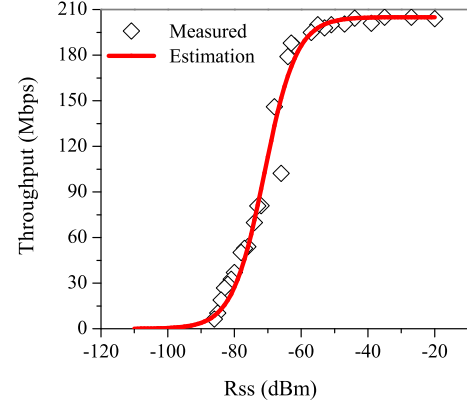
Similarly, from Figure 4.6a and 4.6b, we derived $P_1 = -22.5$, $\alpha = 3.10$, $a = 105$, $b = 43.8$, and $c = 5.2$ for SISO link. They are well coincident with the results in Table 4.2.

Table 4.2: Parameter values with NEC AP for *field#1*.

parameter	P_1	α	a	b	c
MIMO	-20.3	2.85	205	49.0	4.8
SISO	-22.5	3.10	105	43.8	5.2

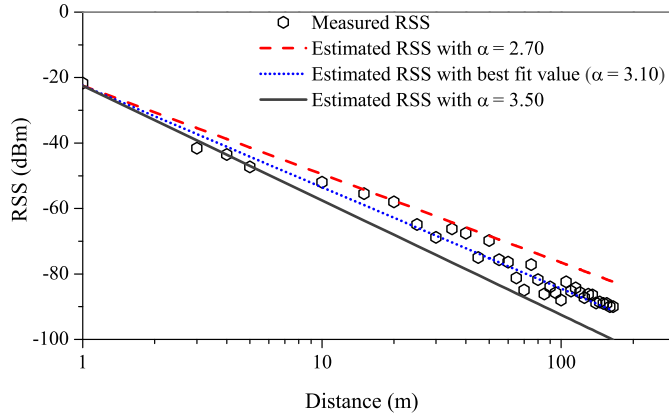


(a) RSS estimation.

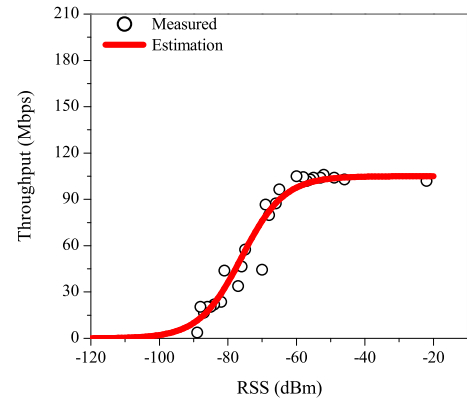


(b) Sigmoid curve for MIMO link.

Figure 4.5: RSS and throughput estimation for 2×2 MIMO link in *field#1*.



(a) RSS estimation.



(b) Sigmoid curve for SISO links.

Figure 4.6: RSS and throughput estimation for SISO link in *field#1*.

3. *Estimation results in outdoor:* For 2×2 MIMO, and 1×1 SISO links, Figure 4.7 shows the throughput estimation results in the *field#1* by the *throughput estimation model* when the distance between the AP and the host is changed from $0m$ to $170m$ with the $5m$ interval. It is noticed that the estimated throughputs are very similar to the measured ones. The throughput estimation results by our model are continuous because it adopts the continuous functions. On the other hand, the throughput results by measurement are stepwise due to the changes of MCS.

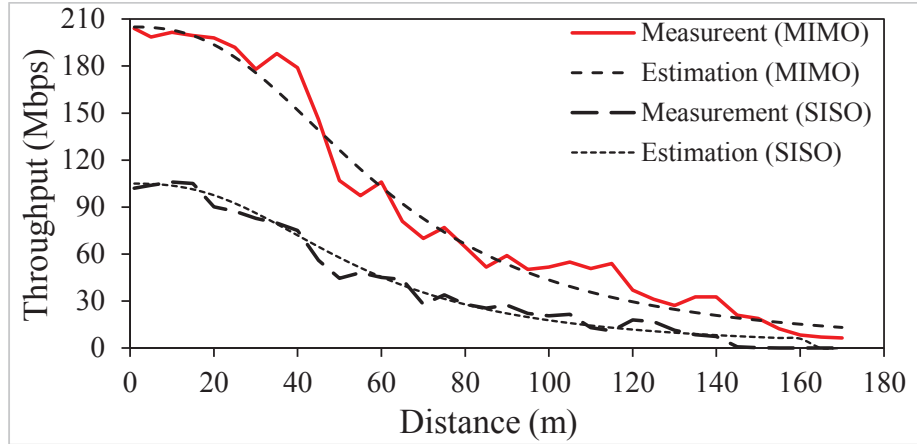


Figure 4.7: Throughput results in *field#1*.

Table 4.3 shows the average (*avg*), maximum (*max*), minimum (*min*), and standard deviation (*STD*) of the throughput estimation errors with respect to the measurement results. These results indicate that our model can give similar throughput estimation results with small errors from the measurement ones.

Table 4.3: Throughput estimation error (Mbps) with NEC AP in *field#1*.

802.11n links	avg	max	min	STD
MIMO	7.27	27.13	0.06	6.73
SISO	3.91	13.19	0.13	2.97

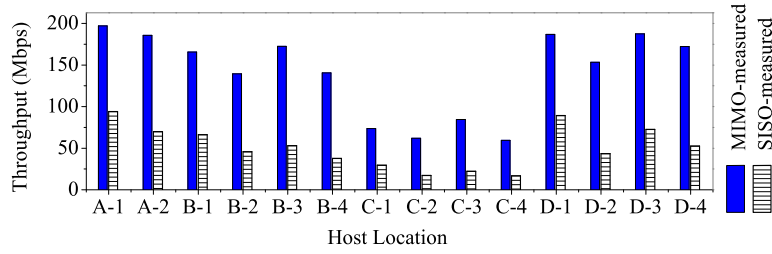
4.3.2 Results in Indoor Environment

Next, we show the throughput results by measurements, and the model in the *field#2* and *field#3* for the indoor environments. Two types of scenarios are considered here: the *line-of-sight (LoS)* scenario at the corridor and the *NLoS* scenario at different host locations in different rooms.

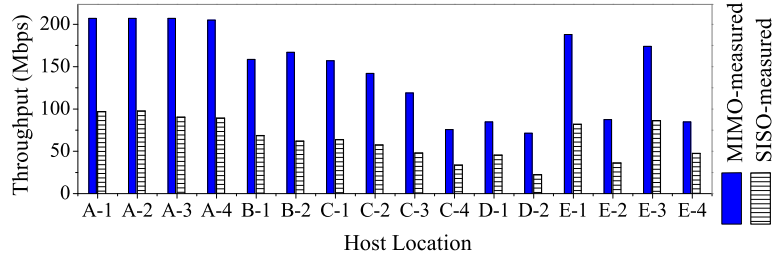
4.3.2.1 Results at Different Hosts Location

A single MIMO/SISO PC is placed at different host locations in Figure 4.2(b) and 4.2(d) to communicate with the NEC AP. It is noted that these AP locations are always fixed and the measurement locations at the host PC can receive the signal from the AP.

- *Measurement Results:* In this experiment, we measured the throughput (*Mbps*) and the RSS (*dBm*) for the 2×2 MIMO link and the 1×1 link, when a single host is placed at 14 different host locations in the *field#2* and 16 locations in the *field#3* as in Figure 4.2(b) and 4.2(d) respectively. Figure 4.8 shows the change of the throughput results with the different host locations for AP1 in the *field#2* and *field#3*. The RSS drops due to the signal attenuations by different types of walls, by the distance between the AP and the host, and the multi-path effect.

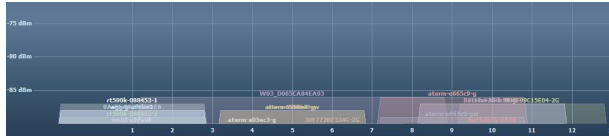


(a) Results for AP1 in *field#2*.

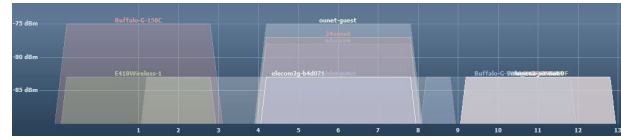


(b) Results for AP1 in *field#3*.

Figure 4.8: Throughput measurement results for 2×2 MIMO and SISO links in indoor fields.



(a) Outdoor channel condition in *field#1*.



(b) Indoor channel condition in *field#2*.

Figure 4.9: Observed channel conditions at 2.4 GHz by Hometown network monitoring tool.

- Model Parameters:** Based on the measurement data in the *field#2* and *field#3*, the values of several parameters namely, P_1 , α , W_k and W_{dif} in Eq. (3.1), (3.2), (3.3), and a , b , and c in Eq. (3.4) for the throughput estimation model for the *IEEE 802.11n SISO* link and the 2×2 *MIMO* link, are optimized by applying the tool. To model complex layouts of several rooms in the *field#2* and *field#3*, the signal attenuation factor W_k is considered for each of the six different walls. They include the *corridor wall* (W_1), the *partition wall* (W_2), the *intervening wall* (W_3), the *glass wall* (W_4), the *elevator wall* (W_5), and the *door wall* (W_6). Table 4.4 shows the optimized parameter values of the throughput estimation model for the *field#2* and *field#3*.

Table 4.4: Parameter values with NEC AP for *field#2* and *field#3*.

network fields	802.11n links	P_1	α	W_1	W_2	W_3	W_5	W_6	W_{dif}	a	b	c
field#2	MIMO	-34.0	2.39	7	8	7	2.0	4.7	1.9	190	47	6.5
	SISO	-35.9	2.10	7	7	8	2.9	2.0	2.0	90	55	8.0
field#2	MIMO	-35.2	2.00	7	5	-	-	2.0	1.0	195	40	6.5
	SISO	-34.0	2.04	11	5	-	-	2.6	2.0	98	40	7.7

Figure 4.10 suggests that the sigmoid curve for the throughput estimation model with 2×2 MIMO link in the *field#2*, can represent the relationship between the measured RSS and the throughput for the link between the AP and the 2×2 MIMO host in the *field#2*.

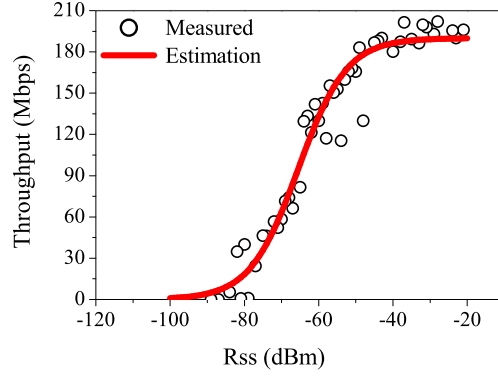


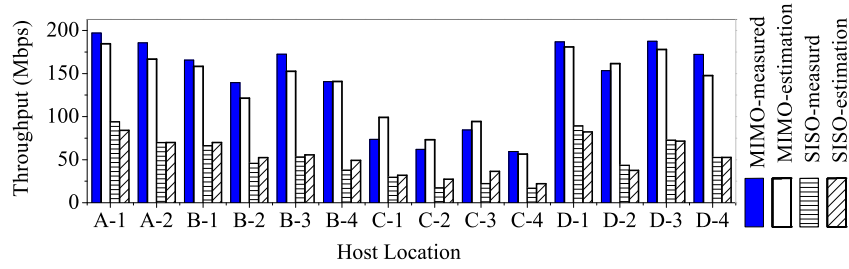
Figure 4.10: Sigmoid curve for 2×2 MIMO link in indoor *field#2*.

- *Estimation results:* Figure 4.11 shows the throughput estimation results in the *field#2* and *field#3* when one host is located at each location in Figures 4.2 (b) and 4.2 (d) respectively.

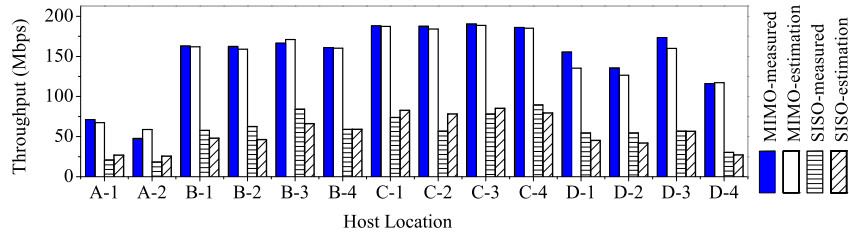
Table 4.5 summarizes the throughput estimation error for the six AP locations in Figure 4.2 (b) and the five AP locations in Figure 4.2 (d) respectively. The estimation error becomes larger than that in the outdoor field, and the accuracy is different depending on the APs or hosts. Especially, the results for some host locations are worse than the others. This reason may come from the insufficiency of modeling the multipath effect in signal propagations and signal attenuations by obstacles in the indoor environment. In addition, during the experiment, some non-target active APs can be observed within usable RSS in the indoor network field as shown in Figures 4.9b, which may cause unwanted interferences for some host locations and result in large estimation errors. This is the truly hard problem. In literature, it has been reported that many simulators do not succeed in accurately modeling them.

Table 4.5: Throughput estimation error (Mbps) with NEC AP in *field#2* and *field#3*.

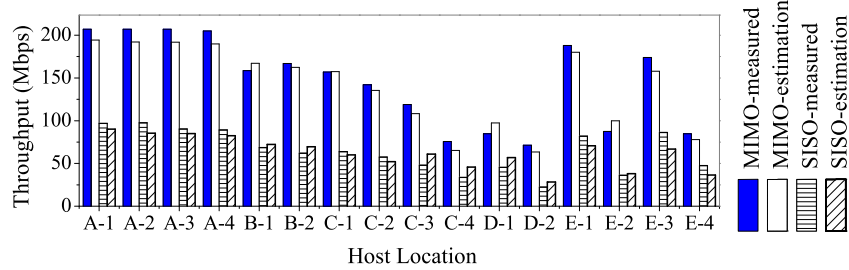
AP ID	802.11n links	field#2				field#3			
		avg.	max.	min.	STD	avg.	max.	min.	STD
AP1	SISO	5.7	14.1	0.01	4.4	8.6	19.5	1.9	4.6
	MIMO	12.5	25.7	0.3	7.8	10.2	16.1	0.4	4.4
AP2	SISO	8.1	19.3	0.9	6.0	5.3	18.8	0.7	5.2
	MIMO	14.9	41.6	4.1	10.9	3.6	15.8	0.1	4.2
AP3	SISO	7.2	21.2	1.4	7.4	4.9	12.0	0.1	3.4
	MIMO	9.1	24.2	0.5	7.0	5.9	10.7	0.1	3.4
AP4	SISO	9.6	24.9	0.5	7.7	4.9	12.3	0.2	3.4
	MIMO	9.1	18.2	0.3	5.7	9.6	29.3	0.4	8.9
AP5	SISO	11.7	24.7	0.03	7.8	7.5	19.8	0.2	6.8
	MIMO	8.4	31.1	0.3	9.1	9.7	21.6	0.5	6.9
AP6	SISO	9.4	21.5	0.04	6.3	-	-	-	-
	MIMO	6.1	20.2	0.7	6.1	-	-	-	-



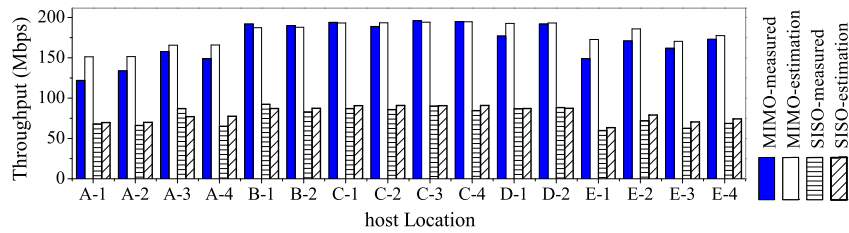
(a) Results for AP1 in *field#2*.



(b) Results for AP6 in *field#2*.



(c) Results for AP1 in *field#3*.



(d) Results for AP4 in *field#3*.

Figure 4.11: Estimation results in indoor fields.

4.3.2.2 Results at Different Distances in Corridor

Here, the AP is placed at the right corner of the corridor (AP1) in the *field#2* in such a way that all the measurement locations for the host PC are capable to achieve the *LoS scenario* from the AP. Seven hosts locations are considered for this scenario where a single 2×2 MIMO host or a SISO host generates TCP traffics to the NEC AP, where the link distance between the host and the AP increases from $0m$ to $30m$ with a separation of $5m$ from each other as shown in Figure 4.2(c).

- **Measurement Results:** First, we present the throughput and RSS measurement results while varying the distance between the AP and the host from $0m$ to $30m$ with the $5m$ interval in the corridor. The AP is located at the $135cm$ height and the MIMO/SISO host is at the $70cm$ height from the 3rd-floor ground. Figure 4.12 shows the results.

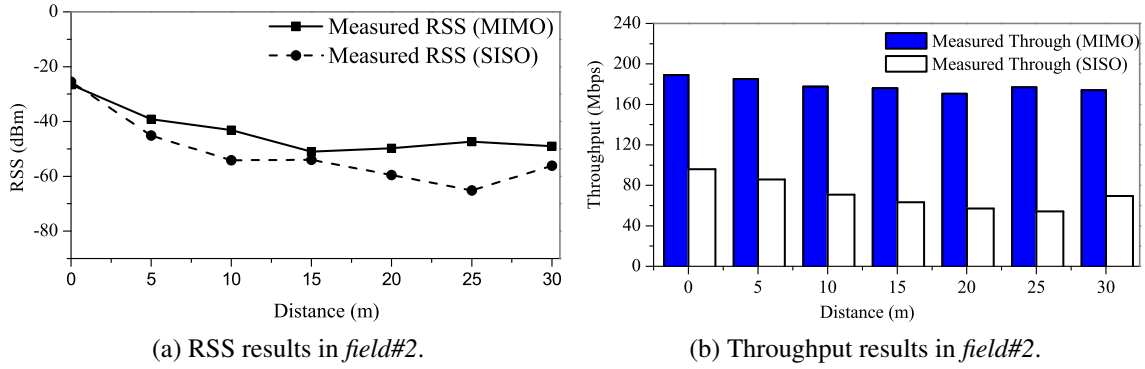


Figure 4.12: Throughput measurement results for different distances at corridor in *field#2*.

In this case, the corridor area acts as a tunnel or waveguide [74] where the wireless signal can propagate without a big loss. As a result, the throughput is not decreased so much as the distance increases, and the throughput performance of the MIMO link is always higher than that of the SISO link. At the distance of 30m at the corridor, the throughput is little increased due to the multipath effect.

- *Estimation results:* Then, the values of model parameters are optimized with the measurement data by the tool. Table 4.6 shows the parameter values for the 2×2 MIMO link and the 1×1 SISO link in the corridor found by the tool.

Table 4.6: Parameter values with NEC AP for corridor in *field#2*.

parameter	P_1	α	a	b	c
MIMO	-27.0	2.32	186	41.3	8.0
SISO	-33.1	2.13	96	54.5	9.0

Figure 4.13 shows the throughput estimation results when the host is located at the seven locations in the corridor. The estimated throughput by the throughput estimation model is very similar to the measured one.

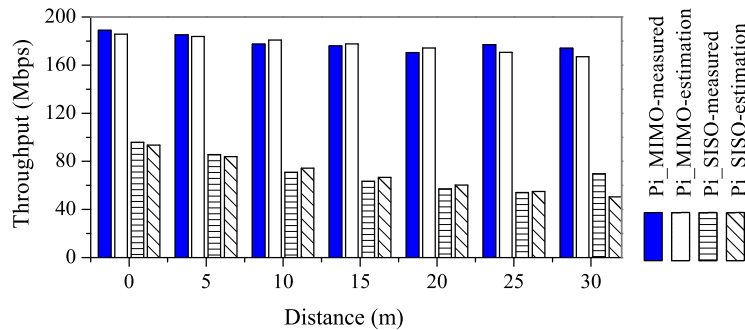


Figure 4.13: Throughput estimation results at corridor in *field#2*.

Table 4.7 shows the average (*avg*), maximum (*max*), minimum (*min*), and standard deviation (*STD*) of the throughput estimation errors at the corridor. These results indicate that our model can give the similar estimation results with small errors from the measurement ones.

Table 4.7: Throughput estimation error (Mbps) with NEC AP at corridor in *field#2*.

802.11n links	avg	max	min	STD
MIMO	3.76	6.90	1.17	2.17
SISO	3.54	10.05	0.74	3.03

4.4 Results for Raspberry Pi AP

In this section, we present the measurement and estimation results of the TCP throughput when *Raspberry Pi* is configured as the software AP using *hostapd* daemon and the built-in NIC adapter. In addition, various external wireless NIC adapters are also used for *Raspberry Pi AP* and their performances are compared. It is noted that the Raspberry Pi internal WiFi module and its driver/firmware capable of MCS7 20MHz channel only [75] where external wireless NIC may useful to support 40MHz.

4.4.1 Configuration of Raspberry Pi for Software AP

Here, the procedure of configuring *Raspberry Pi 3* for the AP with the built-in NIC adapter is briefly presented.

- 1) *hostapd* is installed onto *Raspberry Pi* to give the AP functions by using the command;


```
sudo apt-get install hostapd
```
- 2) *hostapd* is configured using the following steps:
 - i. The configuration file, *hostapd.conf*, is created inside the folder */etc/hostapd/* and is set the necessary configuration options to create the wireless network.
 - ii. To start *hostapd* during the system booting, the absolute path of the configuration file is set by editing inside the folder *etc/default/hostapd/* as


```
DAEMON_CONF="/etc/hostapd/hostapd.conf"
```

 Likewise, run *sudo nano etc/init.d/hostapd/* and find the line *DAEMON_CONF=* and change it to


```
DAEMON_CONF=/etc/hostapd/hostapd.conf
```
- 3) The wireless connection of *Raspberry Pi* is set up to be static by editing the *"/etc/network/interfaces"* file and add the static IP address information.
- 4) The DHCP server is installed to allow the Wi-Fi connection to automatically get the dynamic IP address and DNS etc. by using the command:


```
sudo apt-get install isc-dhcp-server
```

5) The DHCP server is configured using following steps:

- i. *dhcpd.conf* file inside the folder */etc/dhcp/* is edited, and the necessary configuration options are set.
- ii. The wireless adapter as default for the DHCP request is made by editing the */etc/default/isc-dhcp-server* file as
`INTERFACE="wlan0"`

6) Finally, *Network Address Translator (NAT)* is configured by editing the */etc/sysctl.conf* file to enable the IP forwarding. This allows multiple hosts can connect to the AP and have all the data 'tunneled' through the single Ethernet IP.

4.4.2 Results in Outdoor Environments

The throughput estimation results are presented when a single host communicates with the Raspberry Pi AP using its built-in NIC having 1×1 antenna. First, we increase the distance between them from $0m$ to $125m$ along the *LoS scenario* with the $5m$ interval, and measure the throughput at each distance. Then, the parameters values for the throughput estimation model are tuned using the measured data by the tool. The estimation model parameters value are shown in Table 4.8.

Table 4.8: Parameter values with Raspberry Pi AP for *field#1*.

parameter	P_1	α	a	b	c
Raspberry_Pi AP (In-built NIC)	-29.3	2.95	46.0	44.7	6.8

Figure 4.14 shows the throughput measurement results and the estimated ones by the *estimation model* in *field#1*.

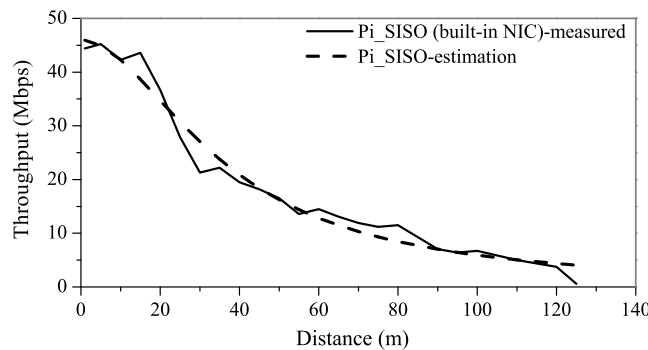


Figure 4.14: Throughput results in *field#1*.

It is observed that the estimated throughputs are very similar to the measured ones. The performance gradually decreases as the distance increases between the AP and the host. The throughput results by measurements are stepwise due to the changes of *MCS* with distance. However, the throughput estimation results by our model are continuous, because it adopts the continuous functions. It is also realized that the peak throughput of Raspberry Pi AP with built-in NIC is around one-half of that for NEC AP with the 1×1 SISO link. In addition, the usable range is also lower than the NEC AP.

Table 4.9 shows the average, maximum, minimum, and standard deviation of the throughput estimation error with respect to the measurement results. These results indicate that our model can give the similar throughput estimation results with small errors to the measurement ones.

Table 4.9: Throughput estimation error (Mbps) with Raspberry Pi in *field#1*.

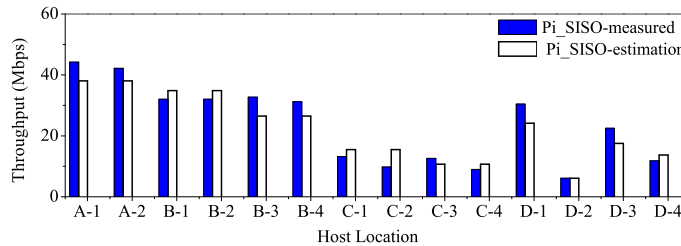
802.11n links	avg	max	min	STD
Raspberry_Pi AP (In-built NIC)	1.54	5.75	0.03	1.53

4.4.3 Results in Indoor Environments

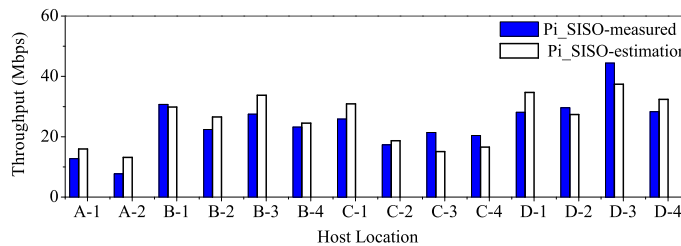
Then, the RSS and throughput measurement results are shown in Figure 4.15 with the estimated results by the *estimation model* when a single host is placed at 14 different host locations in the *field#2* and communicates with the Raspberry Pi AP (built-in NIC).

Table 4.10: Parameter values with Raspberry Pi AP for *field#2*.

	P_1	α	W_1	W_2	W_3	W_5	W_6	W_{dif}	a	b	c
Built-in Pi	-30.6	2.41	10	7	5	2.5	2	2.6	40	56.6	8.5



(a) Results for AP2 in *field#2*.



(b) Results for AP4 in *field#2*.

Figure 4.15: Throughput estimation results for Raspberry Pi AP (built-in NIC) in *field#2*.

Table 4.11 summarizes the throughput estimation errors for the five AP locations in Figure 4.2 (b). The estimation error becomes larger than that in the outdoor field. Particularly, the results for some host locations are little worse. The reason may come from the insufficiency of modeling the multipath effect in the signal propagations and the signal attenuations by obstacles in the indoor environment.

Table 4.11: Throughput estimation error (Mbps) with Raspberry Pi AP in indoor field#2

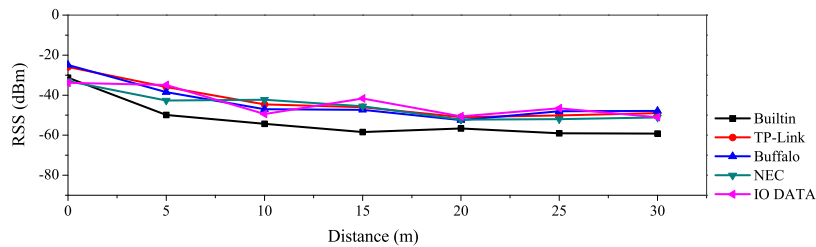
AP	field#2			
	avg.	max.	min.	STD
AP1	4.50	9.87	0.03	3.15
AP2	4.11	12.22	0.05	2.99
AP3	4.24	9.39	0.73	2.32
AP4	4.62	10.31	0.83	2.69
AP5	4.00	12.06	0.02	3.70

4.4.4 Comparisons between Different USB Adapters

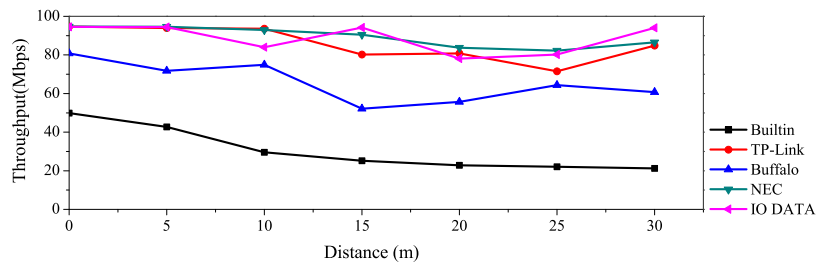
Currently, several external (*USB*) wireless NIC adapters from different vendors are available to improve the throughput performance of Raspberry Pi AP. *TP-Link*, *Buffalo*, *NEC*, and *IO-Data* are popular as the vendors. In this section, we conduct throughput and RSS measurements when the Raspberry Pi AP adopts five different wireless NICs (one in-built adapter, four 2×2 MIMO USB adapters), and compare their performance differences in the *field#2*. The AP is always fixed at the AP1 location in Figure 4.2 (b) and 4.2 (c).

- *Performance Results at Corridor:*

First, the RSS and throughput are measured when a single 2×2 MIMO host communicates with the Raspberry Pi AP in the *LOS scenario* at the corridor in Figure 4.2 (c). The distance between them increases from $1m$ to $30m$ with the $5m$ interval. In this scenario, the AP is placed at the AP1 location in the *field#2* in such a way that all the measurement locations from the host are along LoS from the AP. The Raspberry Pi AP is fixed at $135cm$ height and the 2×2 MIMO host is at $70cm$ height from the 3rd floor ground. Figure 4.16 shows the measurement results.



(a) Distance vs. RSS.



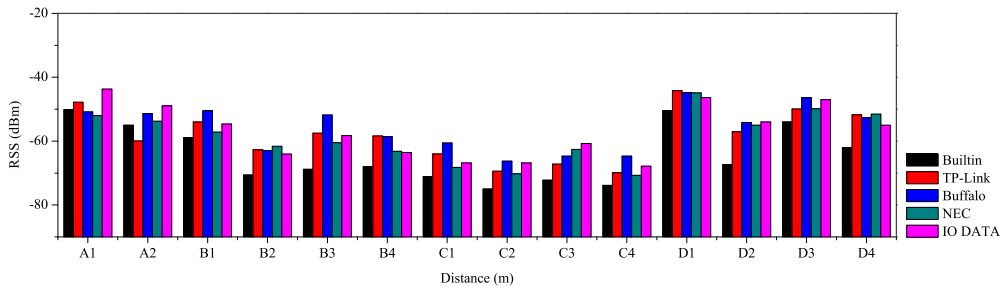
(b) Distance vs. throughput.

Figure 4.16: Performance results at different distances with different USB adapters.

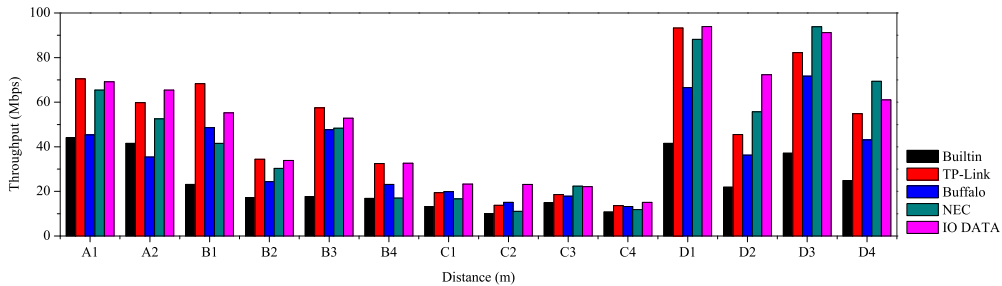
The throughput performance of the Raspberry Pi AP with a USB wireless NIC adapter is always higher than that with the built-in wireless NIC. It is also observed that the total throughput by the *NEC* USB adapter is largest among the USB adapters. Here, the corridor is similar to a tunnel, and the wireless signal propagates without a big loss. As a result, the throughput by any AP is not much decreased as the distance increases, and the throughput by Raspberry Pi AP with *NEC* USB wireless adapter gives the best performance among them.

- *Performance Results at Different Hosts Locations:*

Then, the RSS and throughput are measured when a single 2×2 MIMO host is placed at 14 different host locations in the *field#2* and communicates with the Raspberry Pi AP. In this case, the measurement locations for the host are along NLOS from the AP. Figure 4.17 shows the measurement results. It is observed that the throughput variation occurs among different host locations. In this case, the RSS drops due to the signal attenuation by different types of walls.



(a) Host location vs. RSS.



(b) Host location vs. throughput.

Figure 4.17: Performance results at different hosts location with different USB wireless NIC adapters.

It is also observed that the total throughput by the Raspberry Pi AP with the *IO-Data* USB wireless adapter is the largest among the external wireless adapters. The throughput by the built-in wireless NIC is smallest.

4.5 Throughput Estimation for Concurrent Communication

In this section, we show throughput estimation results when multiple hosts are simultaneously communicating with a single AP as more practical scenarios. First, we measure throughputs of the hosts in the indoor environments. Then, based on throughput measurement results, we propose two

modifications to the throughput estimation model [14] to improve the accuracy for the concurrent communications of multiple hosts in WLAN. Finally, we verify the effectiveness of our proposal in *field#2* and *field#3*.

4.5.1 Experiment Setup

In the experiments, first, we adopt one AP, five SISO hosts and three rooms (A, B, C) in the *field#2*. We considered two cases. In the *one-room case*, one AP is located at the center in room C where all the hosts are uniformly located there. In the *three-rooms case*, the AP is located at the center in the room B, one host is located at the center of room A and two hosts are symmetrically in rooms B and C respectively. Figure 4.18 shows the experiment layout for the two cases, (a) one room, and (b) three rooms, respectively. Then, we also conduct throughput measurements by using the same topology when we adopt one 2×2 MIMO host among five hosts and rests are SISO hosts, where the MIMO host is located either in room A, B, or C.

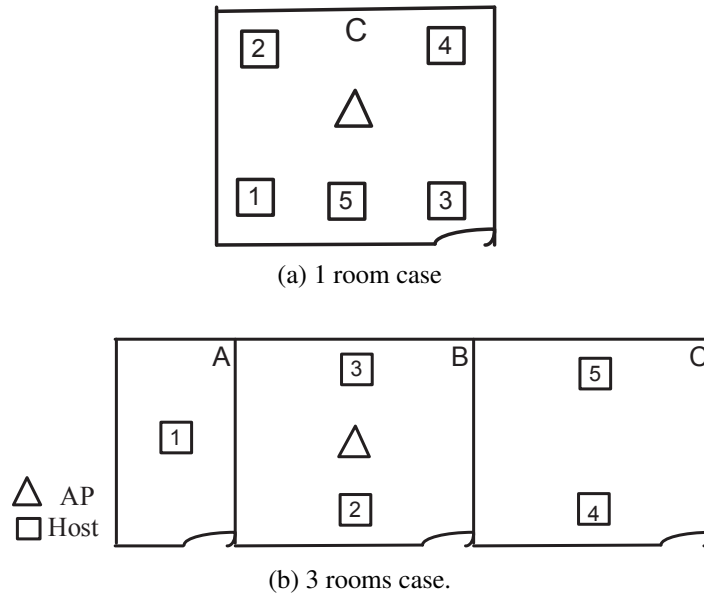


Figure 4.18: Experiment setup for two cases in *field#2*.

Experiments are conducted using six laptop PCs equipped with the *IEEE 802.11n NICs*, where one PC is used for the server and five are for the hosts. One commercial AP *NEC WG2600HP* that supports up to 3×3 MIMO is also used. Before experiments, we disable the unnecessary programs from the PCs and run the *SG TCP optimizer* tool to tune and optimize network adapters. In our experiments, five hosts are simultaneously generating TCP traffics to the AP and *iperf 2.05* is used to measure the throughput. Each measurement is repeated five times to take the average results.

4.5.2 Measurement Results

First, we show the throughput measurement results for both one-room and three-rooms case..

4.5.2.1 Measurement Results for one-room case

Figure 4.19 shows the total throughput and individual host throughput measurement results when 5 SISO hosts are concurrently communicating with one AP. From Figure 4.19a, it is observed that the total throughput decreases significantly with the number of concurrent communicating hosts per AP, since the packet errors occur due to concurrent activation of multiple links which decrease their transmission speed. From Figure 4.19b, it is also observed that the throughput of each host is nearly similar although some small fluctuations occur due to the design of WiFi adapters and the backoff mechanisms.

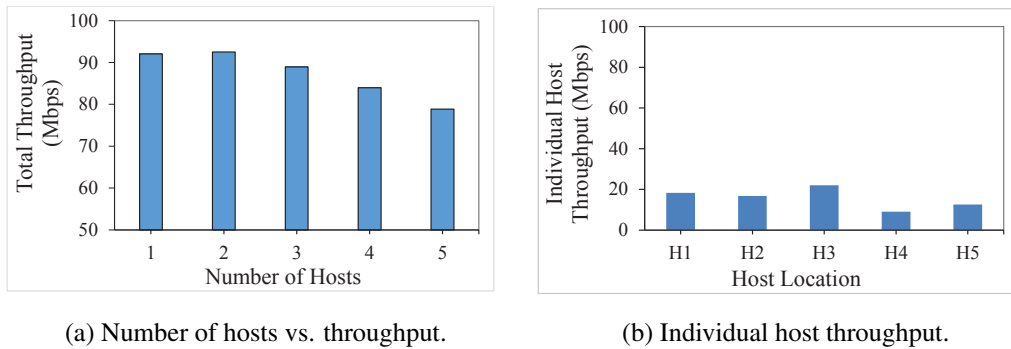


Figure 4.19: Throughput results for one-room case in *field#2*.

4.5.2.2 Measurement Results for three rooms case

For three rooms case, the total throughput also declines with the number of concurrent communicating hosts per AP as shown in Figure 4.20a. In this case, the throughput of same room hosts (H2, H3) as the AP is much higher than expected. On the other hand, different room hosts (H1, H4, H5) throughput is much lower than expected as in Figure 4.20b. Because, during concurrent communication, only closer host to the AP gets much higher transmission chance by stronger RSS and the AP can still successfully receive a packet from the strongest RSS despite significant interference from other hosts.

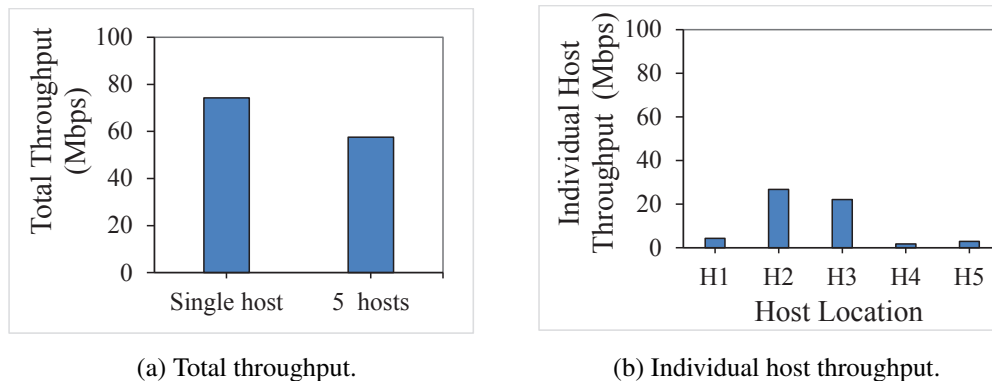


Figure 4.20: Throughput results for three-rooms case in *field#2*.

Table 4.12 shows measured throughputs (*Mbps*) for the five hosts in two cases. It is noted that when multiple hosts are concurrently communicating with one AP, their throughputs are often not

fair. In the MAC protocol, the *fragmentation burst* is combined to increase the throughput by reducing overheads in the backoff mechanism for contention resolutions [3]. As a result, some hosts may occupy the frequency channel for a long time, which results in imbalanced throughput results among the hosts. Therefore, the total throughput of the five hosts is evaluated in our experiments. Table 4.12 also shows the total estimated throughput by the original model with the *WIMNET simulator* [28]. Unfortunately, it is found that the estimated throughput by the original model is not proportional to the measured one.

Table 4.12: Throughput results (Mbps) for multiple links (only SISO) in *field#2*.

room case	measure-ment	original model	hypothesis		
			1)	2)	1) & 2)
(a)	78.84	85.74	75.79	-	-
(b)	57.59	65.59	57.49	72.78	62.31

4.5.3 Model Modifications

To improve the accuracy of the throughput estimation model under concurrent communication of multiple hosts, the following two *hypotheses* are considered:

- *Hypothesis-1)*
The contention resolution mechanism in the MAC protocol sometimes do not work properly between two or more links communicating with the same AP due to the random backoff time. This hypothesis can increase packet errors due to simultaneous activations of multiple interfering links, which decreases their transmission speeds.
- *Hypothesis-2)*
The hosts closer to the AP can take more transmission chances than the farer hosts due to the stronger RSS, the higher transmission speed, and the large TCP window size. This hypothesis can increase the transmission speeds of the links with the closer hosts to the AP than the expected ones among the multiple interfering links.

Then, we present two modifications to the throughput estimation model to reflect these hypotheses as follows:

1. The transmission speed or throughput of each link is modified by multiplying with a factor from the one obtained by the *sigmoid function* s (Mbps) in the original model to reflect Hypothesis-1), as in [17].

$$s = \frac{a}{1 + e^{-\left(\frac{P_d+120}{c}\right)-b}} * f(x) \quad (4.1)$$

where $f(x)$ represents the throughput reduction factor and x does the number of concurrent communicating hosts per AP. The throughput reduction factor $f(x)$ is derived by fitting it with the measured data as:

$$f(x) = 1 - 0.1 * (x - 1)/4; f(5) = 0.9; \quad (4.2)$$

Figure 4.21 confirms the accuracy of this reduction factor.

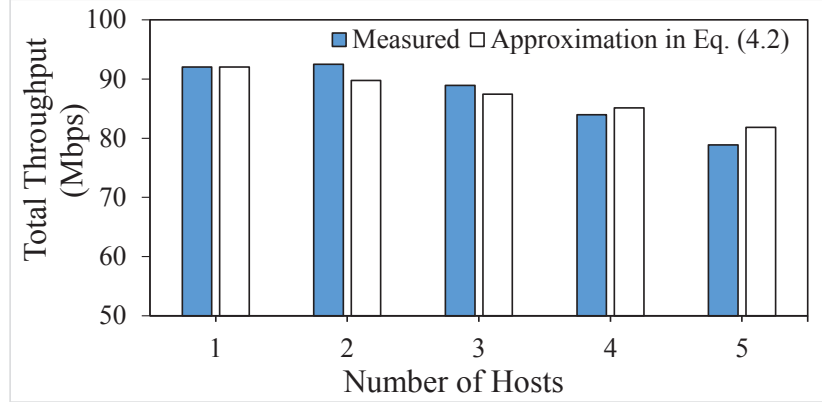


Figure 4.21: Throughput estimation with reduction factor.

2. The transmission chance of the host in the same room as the AP is increased by a constant factor over the host in the different room, to consider Hypothesis-2). As a result, the host in the same room as the AP achieves the higher transmission speed than the expected one by the throughput estimation model due to the large TCP window size, and the host in the different room from the AP achieves the lower transmission speed.

In our model modification, we introduce the number of host replicas to reflect the difference of transmission chances among the hosts. Let r_{jk} be the number of host replicas. In this thesis, it is derived from our measurement results as:

$$r_{jk} = \begin{cases} 7, & \text{for the host in the same room as the AP} \\ 1, & \text{otherwise} \end{cases} \quad (4.3)$$

Figure 4.22 shows the idea of the host replicas in the second model modification.

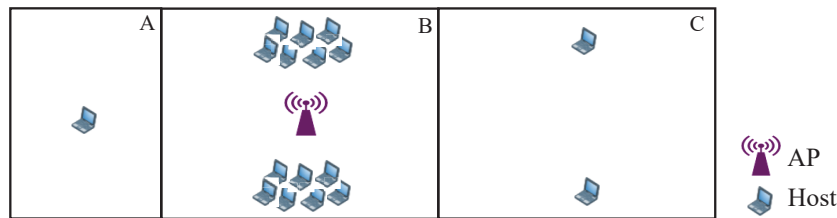


Figure 4.22: Host replicas for second model modification.

Then, the estimated average host throughput TH_j for the j th AP is modified as:

$$TH_j = \frac{\sum r_{jk}}{\sum_{k \in H_j} \frac{r_{jk}}{s_{jk} \cdot f(|H_j|)}} \quad (4.4)$$

where H_j is the set of hosts associated with AP_j and s_{jk} is the throughput between AP_j and $host_k$.

4.5.4 Evaluation Results

Figure 4.23 shows the throughput estimation results in the *field#2* by the *modified throughput estimation model*, which are compared with the results by the *original model*. It is observed that the total estimated throughput after the two modifications in Table 4.12 fits well with the measured one in any case, and has the better accuracy than the *original model*.

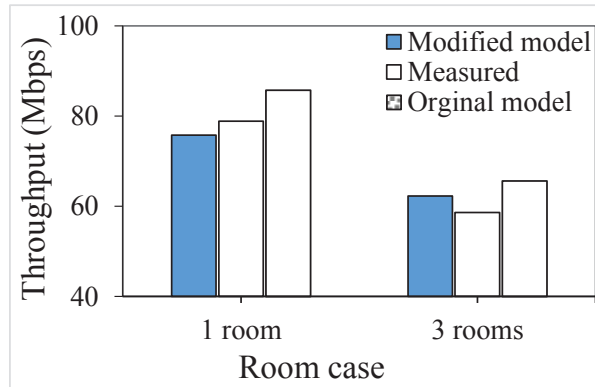


Figure 4.23: Evaluation results of the proposed model for SISO links in *field#2*.

Then, we evaluate our proposal when we adopt one MIMO and four SISO hosts using the same topology as the previous one where the MIMO host is either in room A, B or C. Figure 4.24 shows the throughput estimation results in the *field#2* by the *modified model* and the *original model*, which are compared with the measured results. It is observed that the total estimated throughput after the two modifications in Table 4.13 fits well with the measured one in any case, and has the better accuracy than the *original model*.

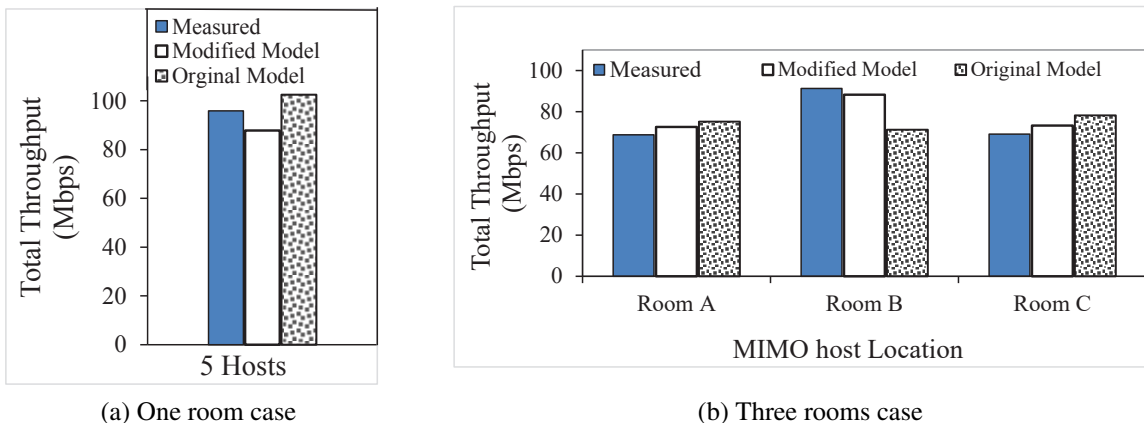


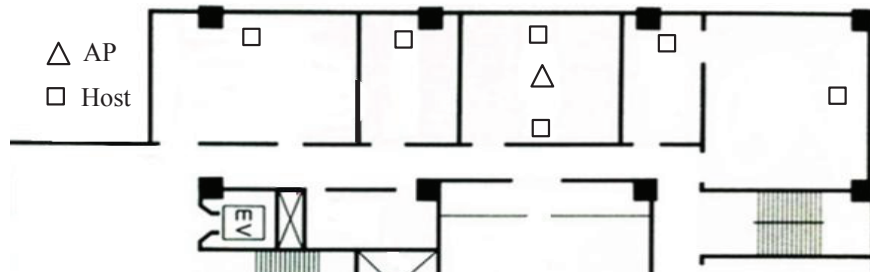
Figure 4.24: Evaluation results of proposed model for MIMO and SISO links in *field#2*.

Finally, we evaluate the performance of the throughput estimation model using a larger network scenario, where one NEC AP and six hosts (one MIMO, and five SISO) are distributed in five rooms (A, B, C, D, E) separated by walls with different types of walls in the *field#3*, as shown in Figure 4.25a. Throughputs are estimated before and after applying the proposed modifications. It is observed that the estimated throughput with the modified model fits well with the measured

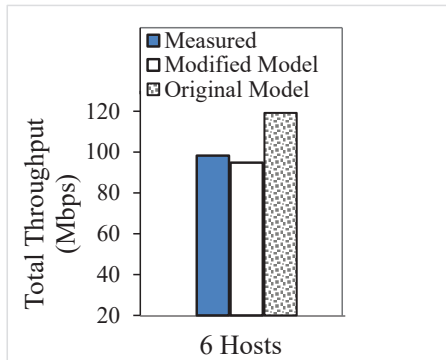
Table 4.13: Throughput results (Mbps) for multiple links (MIMO and SISO) in *field#2*.

room case	MIMO host	measurement	original model	hypothesis		
				1)	2)	1) & 2)
(a)	C	95.89	102.52	87.85	-	-
(b)	A	68.76	75.20	66.97	82.71	72.61
(b)	B	91.29	71.26	63.92	99.93	88.79
(b)	C	69.08	78.22	69.93	83.51	73.29

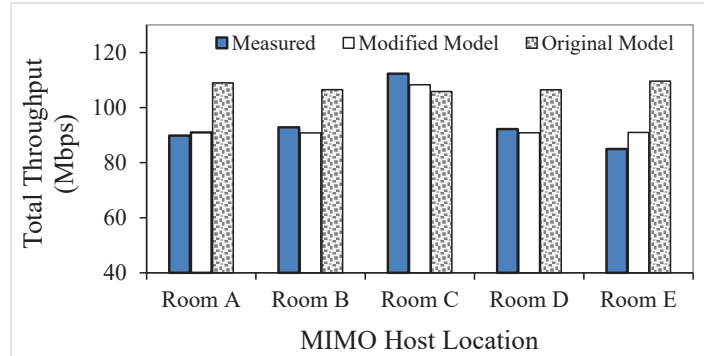
result in any case and also has the better accuracy than the *original model* as shown in Figure 4.25b and Figure 4.25c.



(a) Network topology in graduate school building (*field#2*)



(b) One room case



(c) Five rooms case

Figure 4.25: Evaluation results for proposed model for MIMO and SISO links in *field#3*.

4.6 Summary

In this chapter, we first presented the throughput and RSS measurement results for commercial APs and software APs with IEEE 802.11n MIMO/SISO links under various conditions in indoor and outdoor environments. The results show that the throughput and RSS are strongly affected by the type of the AP or PC model, the link distance between the AP and the host, the AP and host locations, and the network environment. Then, we investigated the accuracy of throughput

estimation results by the throughput estimation model when a single host is communicating with the AP at a time. The results indicate that our model can estimate the throughput with considerably high accuracy with the small error from the measured results. We also verify that for throughput estimation of MIMO link, same model but different parameter values are acceptable.

Next, we compared throughput performances among various wireless NIC adapters for the Raspberry Pi AP.

Besides, we proposed two modifications to the throughput estimation model to improve the estimation accuracy for concurrent communications when multiple hosts are simultaneously communicating with the same AP. The throughput estimation results in two network fields have verified the effectiveness of the proposal.

In the next chapter, we will propose the *MIMO host location optimization approach* for the active AP configuration algorithm.

Chapter 5

Proposal of MIMO Host Location Optimization Approach

In this chapter, we present the *MIMO host location optimization approach* as an extension of the *active AP configuration algorithm* for the *elastic WLAN system*. First, we describe the background of this proposal. Then, we formulate the MIMO host location optimization problem to design the algorithm. Finally, we describe the procedure for the MIMO host location optimization algorithm for the elastic WLAN system.

5.1 Introduction

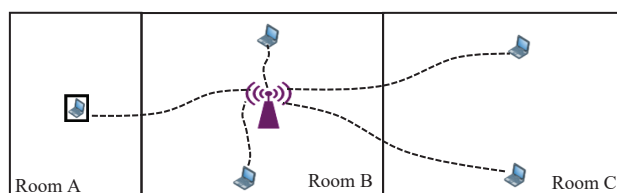
In Chapter 3, we presented the review of the previous studies of the active AP configuration algorithm for the elastic WLAN system. This algorithm can dynamically optimize the number of active APs depending on traffic demands and network situations [11, 12]. The elastic WLAN system is targeting the *indoor network environment*, which consists of several rooms for offices, laboratories, or classrooms in a building, because WLANs are usually deployed there. WLAN users normally use personal computers (PCs) to access the Internet at fixed positions where chairs and tables are available, and access the Internet while sitting on chairs and putting their PCs on tables, because PCs are much larger and heavier than smartphones, and often require the use of both hands. As a result, the mobility of WLAN users is much lower than that of the cellular system users. In such cases, the possible locations of the hosts can be determined by the locations of desks and chairs and can be fixed.

In the current active AP configuration algorithm, it is assumed that each AP and host only use IEEE 802.11n *SISO (Single-Input-Single-Output)* link for wireless communications under the assumption of a single host communication with the AP at a time, although *MIMO (Multiple-Input-Multiple-Output)* has become available as the faster communication technology among commercial AP devices and PC models. MIMO can use multiple data streams by adopting multiple antennas. Currently, in WLAN, nearly all the commercial APs can use MIMO, but only a subset of hosts may use MIMO, because PCs with MIMO are more expensive than PCs with SISO. In this thesis, a host that can use MIMO is called a *MIMO host* and a host that can only use SISO is called a *SISO host* for convenience. To improve the network performance, it is important to find the optimal locations of the limited MIMO hosts in the network field that can optimize the ability of MIMO host communication. At the same time, the concurrent communication effect of multiple hosts with a single AP is more realistic, which should be considered.

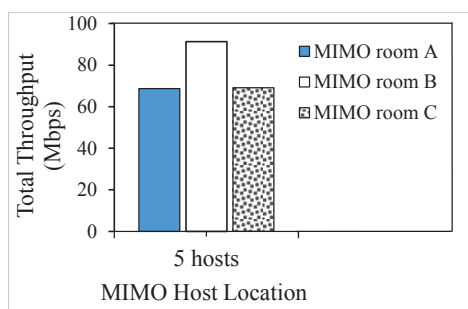
As a practical application of this proposal, if the network manager can control the locations of the hosts, he/she can assign the locations of the MIMO hosts by following the proposed algorithm output. For example, a computer exercise room and a student laboratory in a university or a cyber-cafe can be this case. If the network manager cannot control them, still, he/she can encourage the MIMO host users to move to the locations that are specified by the algorithm output by showing the instructions or giving some incentives such as discounts at the use of WLANs.

5.2 Motivation of MIMO host location optimization

In our preliminary throughput measurement using a small network scenario in Figure 5.1a with one MIMO and four SISO hosts (where MIMO host is either in room A, B or C), we observe that MIMO host in room B (same room as the AP) provides much higher throughput results than other cases as shown in Figure 5.1b.



(a) Simple network topology



(b) Throughput results

Figure 5.1: Throughput results with one MIMO and four SISO links.

Therefore, the proper locations of MIMO host become important to optimize the performance of the network by maximizing the potential ability of MIMO communication.

5.3 Proposal of MIMO host location optimization algorithm

In WLAN, it is common that hosts often join/leave to/from the network, and network conditions can be changed in the long term. To deal with these practical situations, the active AP configuration algorithm has been studied in the two phases. The algorithm for the first phase is designed to find the initial setup of the whole network where the topology configuration of all the APs and hosts in the network can be changed at the same time [9, 12]. It can be used for the design phase of the network or for the reset phase of the topology. The algorithm for the second phase is designed to find the optimal association of a joining host or the optimal re-associations of existing hosts due to a leaving host from the network [76].

In this chapter, we propose an extension of the active AP configuration algorithm for the first phase to optimize the locations of the MIMO hosts in the network under concurrent communication, when all the DAPs use MIMO and a subset of hosts use MIMO. In this extension, the MIMO host locations are optimized by exchanging the locations of randomly selected MIMO hosts with those of randomly selected SISO hosts, if the swapping result can satisfy the constraints of the network and improve the total throughput performance. This random host interchange will be repeated by the given times.

5.3.1 Problem Formulation

The MIMO host location optimization problem for the extension of the active AP configuration algorithm is formulated as a combinatorial optimization problem:

1. **Inputs:**

- Number of hosts: H
- Number of APs: N
- Antenna type of each hosts: *MIMO* or *SISO*
- Antenna type of each APs: *MIMO*
- AP ID: $i = 1$ to N
- Host ID: $j = 1$ to H
- Link speed of the i th AP to the j th host, s_{ij} ($i = 1$ to N , $j = 1$ to H) :, where the link speed can be estimated by the throughput estimation model in [14, 24].

2. **Outputs :**

- Locations of MIMO hosts
- The set of active APs
- The set of the hosts associated with each active AP

3. **Objectives :**

- To minimize the number of active APs E_1
- Holding the first objective, to maximize minimum host throughput among the active APs E_2 .

The cost function E_2 is defined as follows:

$$E_2 = \min_j [TH_j] \quad (5.1)$$

where TH_j represents the average host throughput for the j th AP.

To consider the effect in concurrent communications, the estimated average host throughput TH_j for the j th AP is modified as:

$$TH_j = \frac{\sum r_{jk}}{\sum_{k \in H_j} \frac{r_{jk}}{s_{jk} \cdot f(|H_j|)}} \quad (5.2)$$

where H_j is the set of hosts associated with AP_j . r_{jk} is the number of host replicas to consider the transmission chance increase, where in the thesis, it is 7 for the host in the same room as the AP, and 1 for other hosts. s_{jk} is the throughput between AP_j and $host_k$. $f(x)$ is the throughput reduction factor by the x number of concurrent communicating hosts with the AP and is defined by:

$$f(x) = 1 - 0.1 * (x - 1)/4. \quad (5.3)$$

5.3.2 Algorithm Procedure

The following procedure describes the steps of the MIMO host location optimization algorithm.

1. Calculate the link speed or throughput for each possible pair of an AP and a host using the *throughput estimation model* in [14, 24].
2. Derive the initial solution with the number of active APs ($=E_1$) by the greedy algorithm, and calculate the minimum average host throughput for the bottleneck AP ($=E_2$) for the initial solution.
3. Jointly optimize E_1 and E_2 by the local search method [68].
4. Repeat the following steps in L times for *MIMO host location optimization*:
 - (a) Select one SISO host and one MIMO host randomly.
 - (b) Calculate the new average host throughput by Eq. (5.2) and E_2^{new} by Eq. (5.1) when the two hosts are swapped.
 - (c) When the two hosts are associated with different APs, accept this swap if the following two conditions are satisfied:
 - i. new average host throughput for each AP $\geq G$.
 - ii. sum of new average host throughputs for the two APs \geq previous one.
 - iii. $E_2^{new} \geq$ the previous E_2 .
 - (d) Otherwise (associated with the same AP), accept this swap if the new average host throughput \geq the previous one.
 - (e) Repeat the *MIMO host location optimization*, if locations of *MIMO* hosts are changed.
5. Apply the throughput fairness criterion when the total expected bandwidth exceeds B_a (available bandwidth).
6. Terminate the algorithm when either of the following conditions is satisfied:
 - (a) The minimum host throughput constraint is satisfied.
 - (b) All the APs in the network are activated.

5.4 Summary

In this chapter, we presented the *MIMO host location optimization* extension to the active AP configuration algorithm for the elastic WLAN system. First, we formulated the MIMO host location optimization problem as a combinatorial optimization problem to design the algorithm. Then, we described the procedure for the proposed extension. In the next chapter, we will evaluate the effectiveness of the MIMO host location optimization approach through simulations and simple testbed experiments.

Chapter 6

Evaluation of MIMO Host Location Optimization Approach

In this chapter, we evaluate the proposed *MIMO host location optimization approach* in the active *AP configuration algorithm* through simulations using the WIMNET simulator [28] and simple testbed experiments.

6.1 WIMNET Simulator

The WIMNET simulator simulates least functions for wireless communications of hosts and *access-points (APs)* that are required to estimate the data throughputs and delays of packet transmissions in WLAN. It has originally been developed to evaluate a large-scale *Wireless Internet-access Mesh Network (WIMNET)* [28] with reasonable CPU time on a conventional PC. It consists of multiple APs that can form large WLANs and communicate through wireless links. In the WIMNET simulator, it has considered the use of smart antenna as a generalized technology of the IEEE 802.11n *Multiple-Input-Multiple-Output (MIMO)* link and the *Adaptive Array Antenna (AAA)* which can improve the communication performance efficiently by realizing data streams activation with multiple antennas [78].

The WIMNET simulator needs to select several network field parameters such as the AP and host locations, their associations, the existences of different types of wall obstacles, and the communication channels, in order to model various networking scenarios. A sequence of functions such as host movements, communication request arrivals, and wireless link activations are synchronized by a single global clock called a *time slot*. Within an integral multiple of time slots, a host or an AP can complete one-frame transmission and the acknowledge reception. A different transmission rate can be realized by manipulating the time slot length and the number of time slots for one link activation.

6.2 Network Environments

In this thesis, we consider the *indoor network environment* for evaluations of our proposal. This environment consists of several rooms that can be used for offices, laboratories, or classrooms in a building. It is noted that WLANs are usually deployed in a building. In such an environment, WLAN users normally use personal computers (PCs) to access the Internet at fixed positions where chairs and tables are available. They access the Internet while sitting on chairs and putting their

PCs on tables, because PCs are much larger and heavier than smartphones, and often require the use of both hands. As a result, the mobility of WLAN users is much lower than that of the cellular system users. In such cases, the possible locations of the hosts can be determined by the locations of desks and chairs and can be fixed.

6.3 Model Parameters

For simulations, the *throughput estimation model* in [14] was adopted to estimate the link speed using the IEEE 802.11n SISO link with the 1×1 antenna and the MIMO link with the 2×2 antennas for each pair of an AP and a host in each topology.

The two functions in the throughput estimation model have several parameters that are mentioned in *Eq.* (3.1), (3.2), (3.3), and (3.4) which affect its estimation accuracy. These parameters depend on the specifications of the link such as the number of spatial streams, the channel bonding adoption, and the different types of wall obstacles (based on the material and thickness of walls) along the transmission link between two nodes. In our simulations, three types of walls are considered, namely, the corridor wall (W_1), the partition wall (W_2), and the door wall (W_3). Table 6.1 shows their values used in the simulations. They were obtained by applying the *parameter optimization tool* to our measurement data [14, 21].

Table 6.1: Parameter values for throughput estimation model.

	P_1	α	W_1	W_2	W_3	W_{dif}	a	b	c
MIMO	-34.0	2.39	7	8	4.7	1.9	190	47	6.5
SISO	-35.9	2.0	7	8	2.0	2.0	90	55	8.0

6.4 Hardware and Software

Table 6.2 shows the hardware and software configurations of the PC used in our simulations to evaluate the proposal.

Table 6.2: PC environment for simulation.

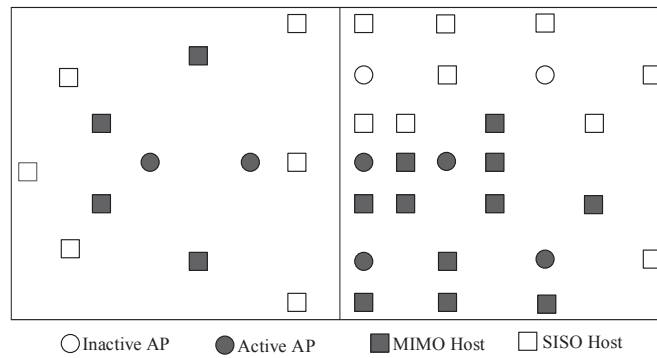
PC model	Lesance W255 HU
processor	Inter(R), Core(TM) i5-2450M (2.50 GHz)
memory (RAM)	4 GB
OS	Ubuntu LTS 14.04, 32 bit

6.5 Evaluation in Random Topology

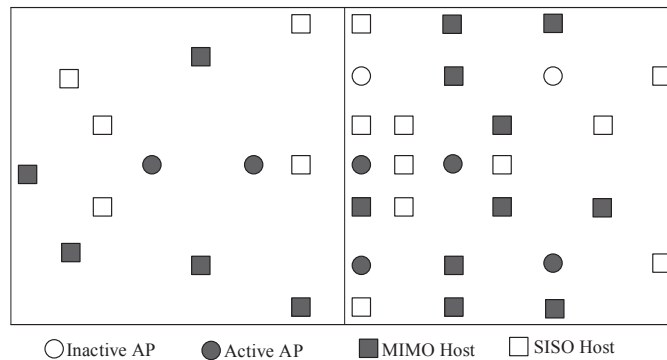
As the first simulation instance, the *random topology* was adopted to evaluate the proposal in a simple network field.

6.5.1 Network Topology

Figure 6.1 (a) illustrates this random topology that is composed of 30 hosts and 8 DAPs in two $400\text{m} \times 200\text{m}$ rooms. In this figure, the gray and white circles represent the active and non-active DAPs, and the gray and white squares imply the MIMO and SISO hosts, respectively. 15 MIMO hosts are randomly selected from the 30 hosts with the 50% probability. The active DAPs are selected by the active AP configuration algorithm where $G = 10\text{Mbps}$ and $B^a = \infty$ are used for the minimum host throughput constraint and the bandwidth limit constraint respectively. Figure 6.1 (b) does the topology after applying the proposed MIMO host location optimization.



(a) before MIMO host location optimization.



(b) after MIMO host location optimization.

Figure 6.1: Random topology for simulations.

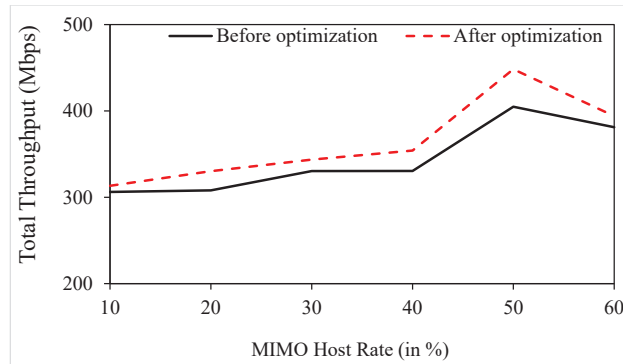
6.5.2 Simulation Results

For the random topology, we investigated the change of the throughput performance when the number of MIMO hosts increased. Table 6.3 and Figure 6.2 demonstrate the number of active APs found by the active AP configuration algorithm, the total throughput of all the hosts before and

after applying the MIMO host location optimization, and the required CPU time. In any case, the proposal improves the total throughput by 5.96% with 3.50% CPU time increase, on average.

Table 6.3: Simulation results for the different number of MIMO hosts in random topology.

MIMO host rate (%)	# of active APs	before optimization		after optimization	
		total throughput (Mbps)	CPU time (s)	total throughput (Mbps)	CPU time (s)
10	6	306.16	5.78	313.28	5.94
20	6	307.97	5.28	330.23	5.49
30	6	330.32	4.41	343.64	4.55
40	6	330.46	4.04	354.12	4.21
50	6	404.85	5.12	448.29	5.31
60	5	381.08	3.66	394.10	3.78



(a) # of MIMO hosts vs. overall throughput.

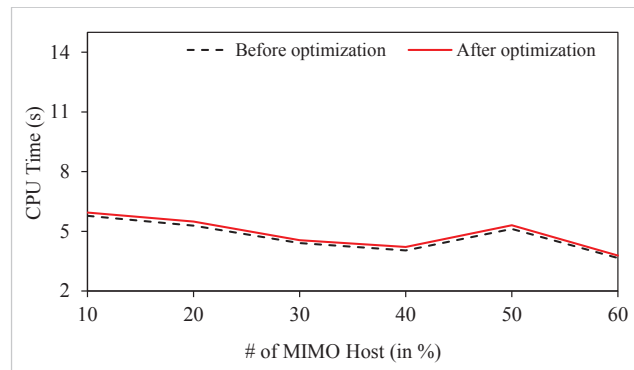


Figure 6.2: Performance graphs for random topology.

6.6 Evaluation in Regular Topology

As the second simulation instance, the *regular topology* was adopted to evaluate the proposal in a complex network field with several rooms.

6.6.1 Network Topology

Figure 6.3 (a) illustrates the regular topology that has 40 hosts and 7 DAPs in six rooms with two different sizes, $7m \times 6m$ and $3.5m \times 6m$. 20 MIMO hosts are randomly selected from the 40 hosts with the 50% probability, and $G = 5Mbps$ and $B^a = \infty$ are used for the algorithm. Figure 6.3 (b) does the topology after applying the MIMO host location optimization.

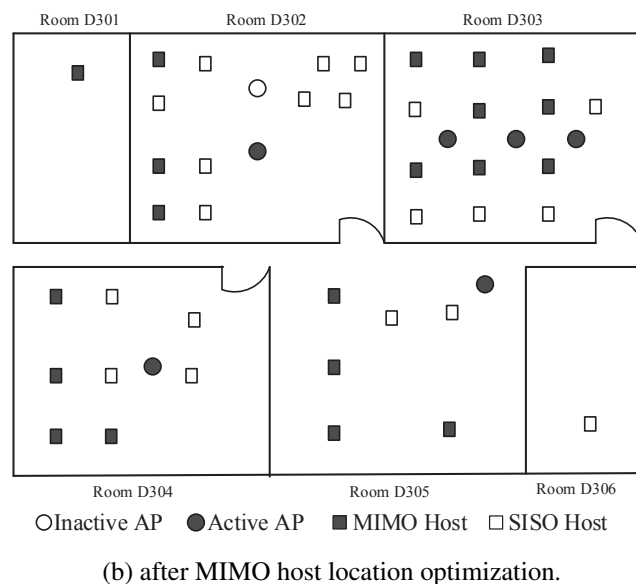
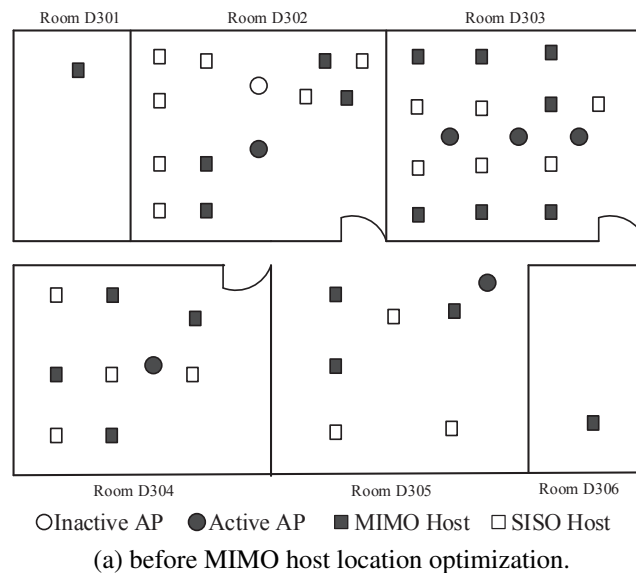


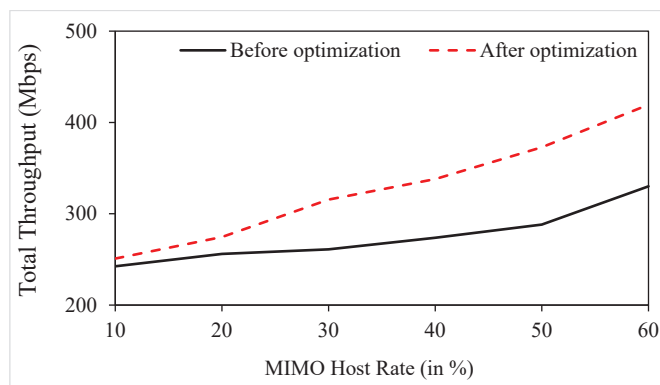
Figure 6.3: Regular topology for simulations.

6.6.2 Simulation Results

For the regular topology, Table 6.4 and Figure 6.4 exhibit the simulation results when the number of MIMO hosts increased in the network field. In any case, the proposal improves the total throughput by 19.36% with 2.86% CPU time increase, on average.

Table 6.4: Simulation results for the different number of MIMO hosts in regular topology.

MIMO host rate (%)	# of active APs	before optimization		after optimization	
		total throughput (Mbps)	CPU time (s)	total throughput (Mbps)	CPU time (s)
10	6	242.48	8.32	250.93	8.62
20	6	255.99	8.28	274.49	8.43
30	6	260.98	8.72	315.49	8.95
40	6	273.69	8.03	338.02	8.31
50	6	288.21	8.07	372.78	8.29
60	6	330.04	8.94	419.35	9.15



(a) # of MIMO hosts vs. overall throughput.

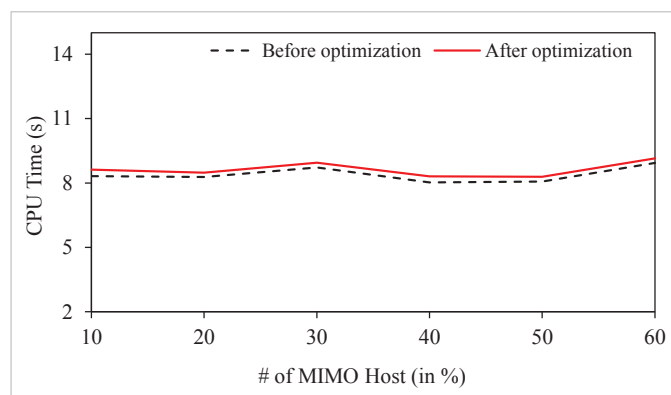


Figure 6.4: Performance graphs for regular topology.

/

6.7 Testbed Experiment Results

Then, a small testbed with one NEC commercial AP and five hosts (one MIMO, four SISO) in three rooms (A, B, C) is considered as a real network environment, in Figure 6.5. The size of room A is $3.5m \times 6m$ and room B or C is $7m \times 6m$. The MIMO host is initially located in either room. Throughputs are measured before and after applying the proposal when the five hosts are concurrently communicating with the AP. They are compared with the simulation results. Table 6.5 shows that both measured and simulated throughputs are improved after the MIMO host location optimization, which confirms the effectiveness of the proposal.

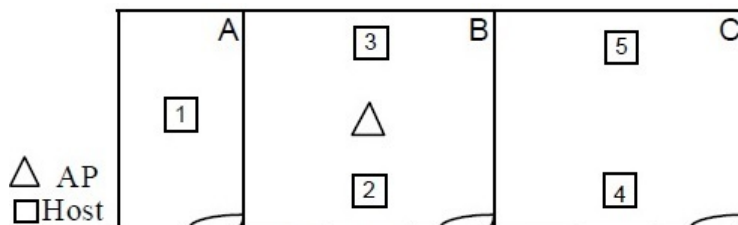


Figure 6.5: Testbed scenario.

Table 6.5: Throughput results.

initial		simulations		
		before optimization	after optimization	
MIMO host room	measured throughput (Mbps)	total throughput (Mbps)	MIMO host room	total throughput (Mbps)
A	68.77	72.61	B	88.72
B	91.29	88.78	B	88.72
C	69.08	73.29	B	88.72

6.8 Summary

In this chapter, first, we introduced the WIMNET simulator and the network environments for simulations and testbed experiments. Then, we showed the throughput estimation model parameters for MIMO and SISO links, hardware, and software used for simulations. Finally, we evaluated the proposal through simulations in two network topologies and simple testbed experiments. The simulation and testbed experiment results confirm its effectiveness by improving the throughput performance by the proposal. In the next chapter, we will conclude this thesis with some future works.

Chapter 7

Conclusion

In this thesis, we presented the studies of the *throughput estimation model* for IEEE 802.11n MIMO and SISO links and the *MIMO host location optimization* approach as the extension of the active AP configuration algorithm for the *elastic WLAN system*.

Firstly, we surveyed the IEEE 802.11 wireless network technologies related to this thesis, including the overview of IEEE 802.11 WLAN, channel access modes in IEEE 802.11 MAC, and its basic backoff mechanism, IEEE 802.11n/ac protocols, link speed change features, the commercial AP, and the software AP using a Raspberry Pi device.

Secondly, we reviewed our previous studies related to this thesis, including the *throughput estimation model*, the *elastic WLAN system*, and the *active AP configuration algorithm*.

Thirdly, we presented extensive measurement results of the *received signal strength (RSS)* and the throughput under a variety of network conditions for use of the throughput estimation of MIMO/SISO links in the MIMO host location optimization. They include commercial APs, software APs with Raspberry Pi, MIMO PCs, SISO PCs, the *single host communication*, and the *concurrent communication* of multiple hosts. The results show that *RSS* and the throughput are strongly affected by the type of the AP, the link distance, and the network field environment. It was observed that the estimated throughput by the throughput estimation model is very similar to the measured result in any case for the single host communication.

Fourthly, we proposed two modifications of the *throughput estimation model* to improve the estimation accuracy under the *concurrent communication* where multiple hosts are simultaneously communicating with one AP. The effectiveness of them was verified by comparing the estimated throughputs with the measured ones in two network fields.

Fifthly, we presented the *MIMO host location optimization* approach as the extension of the active AP configuration algorithm for the *elastic WLAN system*. It repeats to exchange the location of a randomly selected MIMO host with that of a randomly selected SISO host, if the result can improve the total throughput performance.

Finally, we evaluated the effectiveness of the MIMO host location optimization approach through simulations using the *WIMNET simulator* in two network topologies and testbed experiments. The results confirmed the improvement of the throughput performance of the network through comparisons between the outcomes before and after the application of the proposed extension. It was also confirmed that the increase of CPU time is small on average by this extension.

In future studies, we will study further improvements of the throughput estimation model, particularly for concurrent communications between multiple hosts and multiple APs, its evaluations in different network fields, and applications to optimal WLAN designs. We will also study further enhancements of the MIMO host location optimization under the dynamic environment with join-

ing hosts and leaving hosts to/from the network, its implementation into the elastic WLAN system testbed, and investigate the performance evaluations in various network scenarios.

Bibliography

- [1] B. P. Crow, I. Widjaja, J. G. Kim, and P. T. Sakai, "IEEE 802.11 wireless local area networks," *IEEE Commun. Mag.*, vol. 35, no. 9, pp. 116-126, Sept. 1997.
- [2] S. Moghe, and R. Upadhyay, "Comparison of SISO and MIMO techniques in 802.11n wireless local area network," *Proc. Int. Conf. Emerging Trend. Elec. Photonic Devices & Systems (ELECTRO-2009)*, pp. 245-246, Dec. 2009.
- [3] M. S. Gast, *802.11n: a survival guide*, 1st ed., O'Reilly, 2012.
- [4] I. Vermesan, A. Moldovan, T. Palade, and R. Colda, "Multi antenna STBC transmission technique evaluation under IEEE 802.11n conditions," *Proc. 15th Int. Conf. Microwave Techniques (COMITE)*, pp. 51-54, April 2010.
- [5] IEEE 802.11n, Internet: https://en.wikipedia.org/wiki/IEEE_802.11n-2009, Access March 20, 2016.
- [6] D.W. Bliss, K.W. Forsythe, A.O. Hero, and A.F. Yegulalp, "Environmental issues for MIMO capacity," *IEEE Trans. Signal Processing*, vol. 50, no. 9, pp. 2128-2142, Sept. 2002.
- [7] S. Lanzisera, B. Nordman, and R. E. Brown, "Data network equipment energy use and savings potential in buildings," *Energy Efficiency*, vol. 5, no. 2, pp. 149-162, May 2012.
- [8] F. Nadeem, E. Leitgeb, M. S. Awan, and S. Chessa, "Comparing the life time of terrestrial wireless sensor networks by employing hybrid FSO/RF and only RF access networks," *Proc. Int. Conf. Wireless. Mobile Commun. (ICWMC-2009)*, pp. 134-139, Sept. 2009.
- [9] M. E. Islam, N. Funabiki, T. Nakanishi, and K. Watanabe, "An access-point aggregation approach for energy-saving wireless local area networks," *IEICE Trans. Commun.*, vol. E96-B, no. 12, pp. 2986-2997, Dec. 2013.
- [10] M. E. Islam, N. Funabiki, and T. Nakanishi, "Extensions of access-point aggregation algorithm for large-scale wireless local area networks," *Int. J. Netw. Comput.*, vol. 5, no. 1, pp. 200-222, Jan. 2015.
- [11] M. S. A. Mamun, M. E. Islam, and N. Funabiki, "An active access-point configuration algorithm for elastic wireless local-area network system using heterogeneous devices," *Int. J. Netw. Comput.*, vol. 6, no. 2, pp. 395-419, July 2016.
- [12] M. S. A. Mamun, N. Funabiki, K. S. Lwin, M. E. Islam, and W.-C. Kao, "A channel assignment extension of active access-point configuration algorithm for elastic WLAN system and its implementation using Raspberry Pi," *Int. J. Netw. Comput.*, vol. 7, no. 2, pp. 248-270, July 2017.

- [13] Hostapd: the linux way to create virtual Wifi access point, Internet: <http://nims11.wordpress.com/2012/04/27/hostapd-the-linux-way-to-create-virtual-wifi-access-point/>, Access May 20, 2017.
- [14] K. S. Lwin, N. Funabiki, C. Taniguchi, K. K. Zaw, M. S. A. Mamun, M. Kuribayashi, and W.-C. Kao, "A minimax approach for access point setup optimization in IEEE 802.11n wireless networks," *Int. J. Netw. Comput.*, vol. 7, no. 2, pp. 187-207, July 2017.
- [15] A. R. Sandeep, Y. Shreyas, S. Seth, R. Agarwal, and G. Sadashivappa, "Wireless network visualization and indoor empirical propagation model for a campus Wi-Fi network," *World Acad. Sci. Eng. and Tech.*, vol. 42, pp. 730-734, Sept. 2008.
- [16] H. K. Rath, S. Timmadasari, B. Panigrahi, and A. Simha, "Realistic indoor path loss modeling for regular WiFi operations in India," *Proc. National Conf. Commun. (NCC)*, pp. 1-6, March 2017.
- [17] I. Syed, and B. Roh, "Adaptive backoff algorithm for contention window for dense IEEE 802.11 WLANs," *Mobile Inf. Sys.*, pp. 1-11, May 2016.
- [18] G. Hosseinabadi, and N. Vaidya, "Concurrent-MAC: increasing concurrent transmissions in dense wireless LANs," *Proc. Int. Conf. Comput. Netw. Commun. (ICNC)*, pp. 1-5, Feb. 2016
- [19] Z. Hadzi-Velkov and B. Spasenovski, "Capture effect with diversity in IEEE 802.11b DCF," *Proc. Int. Symp. Comp. Commun. (ISCC)*, pp. 699-704, July 2003.
- [20] D. Son, B. Krishnamachari, and J. Heinemann, "Experimental analysis of concurrent packet transmissions in wireless sensor network," *Proc. ACM SenSys Conf.*, pp. 237-249, Nov. 2006.
- [21] S. K. Debnath, N. Funabiki, K. S. Lwin, and M. S. A. Mamun, "A study of throughput estimation model for IEEE802.11n MIMO link in wireless local-area network," *IEICE Tech. Report*, pp. 17-22, Nov. 2017.
- [22] S. K. Debnath, N. Funabiki, K. S. Lwin, M. S. A. Mamun, M. K. Ismael, and M. M. Islam, "Evaluations of throughput estimations in two network simulators for IEEE 802.11n Wireless Local-Area Networks," *Proc. Chugoku-Branch J. Conf.*, Oct. 2017.
- [23] S. K. Debnath, N. Funabiki, K. S. Lwin, M. S. A. Mamun, R. W. Sudibyo, and S. Huda, "Raspberry Pi configuration for access-point and its throughput measurements in IEEE802.11n wireless networks," *IEICE Technical Report*, vol. IEICE-116, no. 382, pp. 101-106, Dec. 2016.
- [24] S. K. Debnath, M. Saha, N. Funabiki, and W.-C. Kao, "A throughput estimation model for IEEE 802.11n MIMO link in wireless local-area networks," *Proc. Int. Conf. Comp. Commun. Syst. (ICCCS-2018)*, pp. 327-331, April 2018.
- [25] N. Funabiki, C. Taniguchi, K. S. Lwin, K. K. Zaw, and W.-C. Kao, "A parameter optimization tool and its application to throughput estimation model for wireless LAN," *Proc. Int. Work. Virtual Environ. Netw.-Orient. Appli. (VENOA)*, pp. 701-710, July 2017.

- [26] S. K. Debnath, N. Funabiki, and M. Saha, "A modified throughput estimation model for concurrent communications in wireless network," IEICE General Conf., March 2018.
- [27] S. K. Debnath, N. Funabiki, M. Saha, M. S. A. Mamun, and W.-C. Kao, "MIMO host location optimization in active access-point configuration algorithm for elastic WLAN system," *Int. J. Space-Base. Sit. Comput.*, (IJSSC), vol. 8, no. 2, pp. 59-69, Aug. 2018.
- [28] N. Funabiki ed., *Wireless mesh networks*, InTech-Open Access Pub., Jan. 2011, Internet: <http://www.intechopen.com/books/wireless-mesh-networks>, Access Jan. 20, 2017.
- [29] Y. A. S. Dama, R. A. Abd-Alhameed, S. Jone, and M. b. Child, "Experimental throughput analysis for 802.11 n system and MIMO indoor propagation prediction," *Proc. Gen. Assem. and Sci. Symp.*, pp. 1-4, Aug. 2011.
- [30] J. Jansons and T. Dorins, "Analyzing IEEE802.11n standard: outdoor performance," *Proc. Int. Conf. Digital Inform. Proc. Commun. (ICDIPC2012)*, pp. 26-30, July 2012.
- [31] C. C. Chew, N. Funabiki, and T. Nakanishi, "Throughput measurements using IEEE 802.11 ac devices for high-speed wireless networks," *IEICE Tech. Rep.*, vol. 113, no. 465, pp. 23-28, Mar. 2014.
- [32] J. Choi, H. Lee, S. Choi, and K. B. Lee, "A Nobel Theoretical Throughput Estimation Method for IEEE 802.11 WLANs," *IEEE Global Commun. Workshops (GC Wkshps)*, pp. 5035-5040, Dec. 2013.
- [33] T. Vanhatupa, M. Hannikainen, and T. D. Hamalainen, "Evaluation of Throughput Estimation Models and Algorithms WLAN Frequency Planning," *Computer Networks*, vol. 51, no. 11, pp. 3110-3124, Aug. 2007.
- [34] R. Bruno, M. Conti, and E. Gregori, "Throughput analysis and measurements in IEEE 802.11 WLANs with TCP and UDP traffic flows," *IEEE Trans. on Mobile Comput.*, vol. 7, no. 2, pp. 171-186, Feb. 2008.
- [35] D. Son, B. Krishnamachari, and J. Heidemann, "Experimental study of the effects of transmission power control and blacklisting in wireless sensor networks," *1st IEEE Commun. Soci. Conf. on Sensor and Ad-Hoc Commun. and Netw.*, pp. 289-298, Oct. 2004.
- [36] X. Ling and K. L. Yeung, "Joint access point placement and channel assignment for 802.11 wireless LANs," *IEEE Trans. Wireless Commun.*, vol. 5, no. 10, pp. 2705-2711, Oct. 2006.
- [37] A. Eisenblatter, H.-F. Geerdes, and I. Siomina, "Integrated access point placement and channel assignment for wireless LANs in an indoor office environment," *Proc. WoWMoM*, 2007.
- [38] I. Koukoutsidis and V. A. Siris, "Access point assignment algorithms in WLANs based on throughput objectives," *Proc. WiOPT*, 2008.
- [39] A. M. Gibney, M. Klepal, and D. Pesch, "A wireless local area network modeling tool for scalable indoor access point placement optimization," *Proc. SpringSim*, April 2010.
- [40] L. Arya and S. C. Sharma, "Coverage and analysis of obstructed indoor WLAN using simulation software and optimization technique," *Proc. CAC2S*, pp. 631-637, 2013.

- [41] M. S. Gast, 802.11 wireless networks, 2nd ed., O'Reilly, 2005.
- [42] S. Banerji, and R. S. Chowdhury, "On IEEE 802.11: wireless LAN technology," *Int. J. Mobi. Net. Commun. & Telematics*, vol. 3, no. 4, Aug. 2013.
- [43] K. Shi, Y. shu, and J. Feng, "A MAC layer congestion control mechanism in IEEE 802.11 WLANs," 4th Int. Conf. on Commun. and Netw., (ChainaCom-2009), pp.1-5, Aug. 2009.
- [44] S. Banerji, "Upcoming standards in wireless local area networks," *Wireless & Mobile Technol.*, vol. 1, no. 1, Sept. 2013.
- [45] I. Poole, "IEEE 802.11 Wi-Fi standards," Internet: <http://www.radio-electronics.com/info/wireless/wi-fi/ieee-802-11-standards-tutorial.php>, Access May 20, 2018.
- [46] V. Beal, "What is 802.11 wireless LAN standards?," Internet: http://www.webopedia.com/TERM/8/802_11.html, Access May 20, 2018.
- [47] "IEEE 802.11 - Wikipedia," Internet: http://en.wikipedia.org/wiki/IEEE_802.11, Access May 20, 2018.
- [48] C. C. Choon, "A study of active access-point selection algorithm for wireless mesh network under practical conditions," Ph.D. thesis, Grad. Sch. Natural Sci. Technol., Okayama Univ., Japan, Sept. 2015.
- [49] M. E. Islam, "A study of access-point aggregation algorithm for elastic wireless local-area network system and its implementation," Ph.D. thesis, Grad. School of Natural Science and Technology, Okayama Univ., Japan, March 2016.
- [50] S. Sendra, M. Garcia, C. Turro, and J. Loret, "WLAN IEEE 802.11 a/b/g/n indoor coverage and interference performance study," *Int. J. Adv. Netw. Service.*, vol. 4, no. 1, pp. 209-222, 2011.
- [51] A. S. Tanenbaum, and D. J. Wetherall, *Computer networks*, 5th ed., Pearson Prentice Hall, 2011.
- [52] J. H. Yeh, J. C. Chen, and C. C. Lee, "WLAN standards," *IEEE Potentials*, vol. 22, no. 4, 2003.
- [53] IEEE, "IEEE Std 802.11-2012, IEEE standard for Information technology," Internet: <https://standards.ieee.org/findstds/standard/802.11-2012.html>, Access May 20, 2018.
- [54] O. Bejarano, E. W. Knightly, and M. Park, "IEEE 802.11ac: from channelization to multi-user MIMO," *IEEE Comm. Mag.*, vol. 51, no. 10, pp. 84-90, Oct. 2013.
- [55] L. Verma, M. Fakharzadeh, and S. Choi, "Wifi on steroids: 802.11ac and 802.11ad," *IEEE Trans. Wireless Comm.*, vol. 20, no. 6, pp. 30-35, Dec. 2013.
- [56] M. S. Gast, 802.11ac: a survival guide, 1st ed., O'Reilly, 2013.
- [57] "WiMAX page, IEEE802.11ac works," Internet: <http://123-info.net/wimax-page/archives/918>, Access May 22, 2018.

- [58] L. Deek, E. Garcia-Villegas, E. Belding, S. J. Lee, and K. Almeroth, "The impact of channel bonding on 802.11n network management," Proc. Conf. Emer. Netw. Exp. Tech. (CoNEXT), Dec. 2011.
- [59] "IEEE 802.11n-2009 - Wikipedia," Internet: http://en.wikipedia.org/wiki/IEEE_802.11n-2009, Access Dec. 20, 2015.
- [60] E. Perahia, and R. Stacey, Next generation wireless LANS: 802.11n and 802.11ac, Cambridge Univ. press, Cambridge, May 2013.
- [61] "IEEE 802.11ac-2008 - Wikipedia," Internet: https://en.wikipedia.org/wiki/IEEE_802.11ac, Access July 25, 2017.
- [62] NEC Inc., "WG2600HP manual," Internet: <http://www.aterm.jp/support/manual/pdf/am1-002673.pdf>, Access Dec. 10, 2015.
- [63] Buffalo Inc., "AirStation WZR-1750DHP user manual," Internet: http://manual.buffalo.jp/buf-doc/35013154-01_EN.pdf, Access Aug. 13, 2016.
- [64] IO data Inc., Internet: <http://www.iodata.jp/product/network/wlan/wlan-ac1600dgr3/index.htm>, Access Feb. 10, 2017.
- [65] Raspberry Pi, "The official website of the Raspberry Pi project," Internet: <http://www.raspberrypi.org/>, Access Jan. 15, 2016.
- [66] M. Sahani, S. K. Rout, A. K. Sharan, and S. Dutta, "Real time color image enhancement with a high regard for restoration of skin color by using Raspberry Pi," Proc. Int. Conf. Commun. Sig. Process. (ICCSP), pp. 335-339, April 2014.
- [67] D. B. Faria, "Modeling signal attenuation in IEEE 802.11 wireless LANs," Tech. Report, TR-KP06-0118, Stanford Univ., July 2005.
- [68] D. P. Williamson, and D. B. Shmoys, The design of approximation algorithms, Cambridge Univ. Press, April 2011.
- [69] K. Pelechrinis, L. Broustis, T. Salonidis, S. V. Krishnamurthy, and P. Mohapatra, "Design and deployment considerations for high performance MIMO testbeds," Proc. Int. Conf. Wireless Internet (WICON), pp. 245-246, Nov. 2008,
- [70] Wiki, "Raspberry Pi 3 Model B," Internet: http://wiki.seedstudio.com/Raspberry_Pi_3_Model_B/, Access Jan. 15, 2016.
- [71] ACD.net, Iperf Speed Testing, Internet: http://support.acd.net/mediawiki-1.16.0/index.php?title=Iperf_Speed_Testing, Access Dec. 13, 2015.
- [72] Software Verzeichnis development, Homedale WLAN Monitor, Internet: <http://www.the-sz.com/products/homedale>, Access March 25, 2017.
- [73] Speed Guide Inc., SG TCP optimizer, Internet: <https://www.speedguide.net/downloads.php>, Access June 10, 2018.

- [74] G. A. Kennedy, and M. D. Bedford, "Underground wireless networking: a performance evaluation of communication standards for tunnelling and mining," *Tunnel. Underground Space Tech.*, vol. 43, pp. 157-170, July 2014.
- [75] RPI3 won't use 40mhz wifi channel width, "Raspberry Pi Forums," Internet: <https://www.raspberrypi.org/forums/viewtopic.php?t=144058>, Access June 24, 2018.
- [76] M. M. Islam, M. S. A. Mamun, N. Funabiki, and M. Kuribayashi, "Dynamic access-point configuration approach for elastic wireless local area network system," *Proc. Int. Symp. Comput. Netw.*, pp. 216-222, Nov. 2017.
- [77] S. Yoshida, N. Funabiki, and T. Nakanishi, "A development of wireless infrastructure mesh network simulator," *Proc. Ad-hoc Workshop*, pp. 1-9, Jan. 2006.
- [78] N. Funabiki, S. Tajima, T. Higashino, T. Nakanishi, and K. Watanabe, "An extension of wireless Internet-access mesh network simulator for use of smart antenna," *Proc. Int. Conf. Broad., Wireless Comput. Commun. Apps.*, pp. 517-522, Nov. 2012.